

1 An ice–climate oscillatory framework for 2 Dansgaard–Oeschger cycles

3 Laurie C. Menviel^{1,†}, Luke C. Skinner², Lev Tarasov³, and Polychronis C. Tzedakis⁴

4 ¹Climate Change Research Centre, PANGEA, University of New South Wales, Sydney, NSW, Australia.

5 ²Department of Earth Sciences, University of Cambridge, Cambridge, UK.

6 ³Department of Physics and Physical Oceanography, Memorial University of Newfoundland, St John's, NL, Canada.

7 ⁴Environmental Change Research Centre, Department of Geography, University College London, London, UK.

8 [†]e-mail: l.menviel@unsw.edu.au

9 ABSTRACT

Intermediate glacial states were characterized by large temperature changes in Greenland and the North Atlantic, referred to as Dansgaard–Oeschger (D–O) variability, with some transitions occurring over a few decades. D–O variability included changes in the strength of the Atlantic Meridional Overturning Circulation (AMOC), temperature changes of opposite sign and asynchronous timing in each hemisphere, shifts in the mean position of the Intertropical Convergence Zone and variations in atmospheric CO₂. Palaeorecords and numerical studies indicate that the AMOC, with a tight coupling to Nordic Seas sea ice, is central to D–O variability, yet a complete theory remains elusive. In this Review, we synthesize the climatic expression and processes proposed to explain D–O cyclicity. What emerges is an oscillatory framework of the AMOC–sea-ice system, arising through feedbacks involving the atmosphere, cryosphere and the Earth's biogeochemical system. Palaeoclimate observations indicate that the AMOC might be more sensitive to perturbations than climate models currently suggest. Tighter constraints on AMOC stability are thus needed to project AMOC changes over the coming century as a response to anthropogenic carbon emissions. Progress can be achieved by additional observational constraints and numerical simulations performed with coupled climate–ice-sheet models.

11 Key points

- 12 • Abrupt warming events in Greenland and the North Atlantic, referred to as Dansgaard–Oeschger (D–O) events, were
13 associated with changes in the strength of the Atlantic Meridional Overturning Circulation (AMOC), global climate and
14 the carbon cycle.
- 15 • AMOC changes, with a tight coupling to Nordic Seas sea ice, strongly affect the climate and marine carbon cycle, and, in
16 turn, ice-sheet mass balance. Resultant changes in oceanic wind stress, ocean heat content and salinity feed back on the
17 AMOC.
- 18 • Owing to the different timescales of the feedbacks, self-sustained AMOC oscillations could emerge during intermediate
19 glacial states. The boundary conditions of intermediate glacial states (size of ice sheets, Bering Strait throughflow and
20 concentration of atmospheric CO₂ appear to be key in enabling these oscillations.
- 21 • Perturbations other than changes in meltwater input, including changes in atmospheric CO₂ or Northern Hemisphere
22 ice-sheet height and extent, can lead to, and may be required for, D–O variability.
- 23 • The relatively large and frequent AMOC changes associated with D–O variability suggest a relatively low AMOC
24 stability during intermediate glacial states. This low stability is not evident in all numerical experiments performed with

25 coupled climate models, implying that some might either overestimate the AMOC stability or have a mismatch in the
26 required background state for the low AMOC stability regime.

- 27 • Additional observations on the location and strength of North Atlantic Deep Water formation and its link with sea ice, as
28 well as its improved representation in climate models, are needed to better constrain future climate projections.

29 [H1] Introduction

30 The Atlantic Meridional Overturning Circulation (AMOC) (Box 1) is a central part of the Earth's climate and biogeochemical
31 system as it transports heat, dissolved salts, nutrients and carbon throughout the ocean's basins. The AMOC is dependent on
32 North Atlantic Deep Water (NADW) formation, which, at present, primarily occurs in the Nordic Seas with a minor component
33 in the Labrador Sea¹. Despite recent weakening², the AMOC has mostly been in a strong state over at least the past 2,000
34 years, and probably most of the Holocene^{3–5}. To a first order, a stable and strong AMOC can be explained by the Stommel
35 salt advection feedback⁶, whereby a strong AMOC is associated with a strong North Atlantic current and thus advection of
36 salty tropical Atlantic waters to the North Atlantic, enhancing deep-water formation at high latitudes. Owing to anthropogenic
37 greenhouse gas emissions, it is likely that the AMOC will weaken over the coming century⁷, with implications for the climate,
38 ecosystems and continental ice sheets. However, there remain significant uncertainties associated with future rates of AMOC
39 changes and the potential of reaching a tipping point, particularly as the AMOC in current coupled climate models has been
40 deemed too stable^{8,9}. It is thus crucial to better understand the processes that affect the AMOC as well as the subsequent
41 response of the climate and carbon cycle.

42 Progress can be achieved by studying past millennial-scale climatic variability (Fig. 1), such as Dansgaard–Oeschger (D–O)
43 cyclicity, during which the AMOC is inferred to have varied substantially¹⁰ (Fig. 1a). First highlighted in Greenland ice cores
44 spanning the last glacial period and deglaciation (~115–11.6 thousand years ago (ka)), D–O cycles are characterized by a
45 decadal-scale air-temperature increase of 5–16 °C in Greenland (a D–O warming event), leading to an interstadial peak (warm
46 conditions)^{11–14} (Fig. 1b). After this interstadial peak, Greenland temperatures gradually decrease over a few centuries to a
47 millennium and then abruptly drop to stadial (cold conditions).

48 Marine sediment cores from the North Atlantic have revealed that some of the D–O stadials identified in Greenland ice
49 cores are associated with thick layers of ice-rafted debris (IRD), inferred to be sourced from fast-flowing terrestrial ice^{15–17}.
50 The majority of these thick IRD layers have a high detrital carbonate content, indicating Hudson Strait provenance¹⁸ and thus
51 implying discharges from the Laurentide Ice Sheet (LIS) and IRD transport by icebergs. These high-IRD episodes are known
52 as Heinrich events and occur within longer cold phases referred to as Heinrich stadials^{19,20}. Twenty five D–O stadials and
53 interstadials have been identified within the last glacial–interglacial cycle, 15 of which occurred during the relatively mild
54 glacial conditions of Marine Isotope Stage 3 (MIS 3; 59.4–24 ka)^{13,14}. By contrast, Heinrich stadials were less frequent, with
55 only six events identified during the last glacial interval and subsequent deglaciation^{18,21} (Fig. 1).

56 D–O cycles and Heinrich events are not restricted to the last glacial period: ice-core and speleothem records suggest
57 prevalent D–O variability over at least the past 800 kyr (ref.²²), and sediment cores from the North Atlantic document IRD
58 layers accompanied by a drop in sea-surface temperature (SST) during glacial periods and deglaciations of the Pleistocene^{21–33}.
59 As evidenced by benthic oxygen isotopic ratio ($\delta^{18}\text{O}$) records, which, to a first order, provide an estimate of the volume of
60 continental ice sheets³⁴, maximum D–O climate variability appears to occur in an intermediate glacial state, when the Northern
61 Hemisphere continental ice sheets are of intermediate size. This intermediate state corresponds to a North Atlantic $\delta^{18}\text{O}$
62 range of 3.5–4.2‰, a globally averaged benthic $\delta^{18}\text{O}$ stack in the range 4–4.7‰ and a relative sea level ~45–80 m lower than
63 present^{25,33,35–37}. Although strict background thresholds for the occurrence of D–O variability are difficult to define precisely,
64 it is clear that D–O variability has generally been suppressed during peak interglacial and peak glacial states²⁵.

65 Palaeoproxy records and numerical simulations provide strong evidence that D–O variability (including Heinrich stadials
66 unless specified otherwise) was associated with changes in the strength of the AMOC^{10,38–40}. These AMOC variations,
67 accompanied by shifts in the seasonal sea-ice extent in the Nordic Seas, Labrador Sea and potentially northern North

68 Atlantic^{41,42}, induced changes in global climate and biogeochemistry^{43–46}. However, the sequence of events and mechanisms
69 that led to D–O climate variability is still highly debated. Each stadial is associated with a higher IRD abundance in the
70 North Atlantic, indicative of enhanced iceberg discharges^{20,25,47–51}. To test the climatic effects of iceberg discharges into the
71 North Atlantic, a freshwater flux is artificially added into the North Atlantic in coupled climate models (termed freshwater
72 hosing experiments)⁵². As the addition of freshwater into the North Atlantic reduces the surface-water density, it weakens
73 deep-water formation and the AMOC, leading to colder conditions over the North Atlantic and Greenland^{52,53}. It was therefore
74 initially suggested that D–O climatic variability is due to the AMOC response to variations in meltwater input into the North
75 Atlantic^{38,47}. However, this hypothesis would mean that the amplitude of stadials (that is, the difference between Heinrich and
76 non-Heinrich stadials) are entirely determined by the magnitude of the forcing. In addition, it has also been suggested that
77 iceberg discharges follow, instead of precede, North Atlantic cooling²⁰. As an alternative to the freshwater hosing proposition,
78 internal oscillations of the ocean–sea-ice system have been suggested⁵⁴. However, these oscillations have been simulated in
79 only a few climate models forced under specific boundary conditions^{55–58}. Abrupt AMOC changes have also been simulated as
80 a response to gradual changes in LIS height⁵⁹ and atmospheric CO₂ concentration⁶⁰. However, the processes leading to these
81 changes in ice sheets, meltwater or CO₂ also need to be constrained and integrated into a D–O framework. To date, no Earth
82 system model has fully replicated all observed climatic and biogeochemical characteristics associated with D–O variability,
83 especially under relevant boundary conditions. D–O variability, including prognostic changes in continental ice sheets and CO₂,
84 remains to be simulated by Earth system models.

85 In this Review, we assess the global climatic changes associated with D–O stadials, Heinrich stadials and interstadials,
86 and the evidence for their link with AMOC changes. We then discuss the possible mechanisms put forward to explain D–O
87 variability and propose a self-sustained oscillatory framework involving all components of the Earth system. Finally, we
88 conclude by considering the implications of the oscillatory framework for AMOC stability.

89 [H1] D–O climatic variability and AMOC changes

90 In this section, we examine the climatic changes associated with D–O variability, as deduced from palaeoproxy records
91 from Greenland and the North Atlantic region, where this climatic variability was first highlighted. We also review the
92 millennial-scale climatic variability that occurs concurrently in distal regions and their link to D–O variability, as revealed by
93 palaeoclimate modelling (Fig. 2). We show that both proximal and distal climatic variability can be explained by variations in
94 AMOC strength in combination with dynamical responses at high southern latitudes and in the North Pacific.

95 [H2] D–O stadials.

96 Greenland ice-core records suggest that the transitions into interstadials are followed by a slow cooling trend, lasting 500 to
97 more than 2,000 years, which ends with a decadal-scale cooling back to stadial conditions⁶¹ (Fig. 1b), with a total temperature
98 change of 6.5–16.5 °C (ref.¹⁴). This cooling is also recorded in the Norwegian Sea, with the spring sea-ice cover advancing
99 to ~62°N^{41,42}, and in the northern North Atlantic, with an equatorward shift of the polar front to ~57°N^{17,20,49,50}. Notable
100 cooling is also recorded over southern Europe^{62–64}, as well as in marine sediment cores from the western Iberian margin and
101 the Mediterranean Sea, with an estimated ~1.5°C decrease in SST during D–O stadials^{26,65,66} (Fig. 1d).

102 Planktonic $\delta^{18}\text{O}$ records reveal the presence of a strong halocline in the Nordic Seas and the northeastern North Atlantic
103 during stadials^{48,67}. It is proposed that these North Atlantic coolings and freshenings, associated with the presence of IRD
104 layers, are linked to AMOC weakening during interstadial to stadial transitions⁴⁷. Furthermore, proxy records indicative of
105 changes in oceanic circulation, such as North Atlantic records of the sedimentary ²³¹Pa/²³⁰Th (refs^{10,68,69}) (Fig. 1a), benthic
106 foraminifera carbon isotope ratio ($\delta^{13}\text{C}$)^{51,70–73}, neodymium isotope ratios (ϵNd)^{68,74,75} and the concentration of carbonate
107 ions ($[\text{CO}_3^{2-}]$) in South Atlantic bottom water⁷⁶, support recurrent AMOC weakening during each stadial of MIS 3.

108 Although the atmospheric poleward heat transport accounts for 78% of the total heat transport at 35°N⁷⁷, the oceanic
109 meridional heat transport in the North Atlantic, with the AMOC being its main contributor⁷⁸ (Box 1), accounts for the total

110 oceanic heat transport north of 30°N. AMOC weakening thus leads to considerable cooling in the North Atlantic and sea-ice
111 advance over the Labrador and Nordic Seas^{53,79} (Fig. 2a). Greater sea-ice cover in the Nordic Seas increases surface albedo
112 and reduces heat loss from the ocean to the atmosphere, thus leading to substantial cooling over Greenland⁸⁰. Paleoproxy
113 records suggest that increased sea-ice cover, reduced air–sea heat exchange and weaker deep-ocean convection could also
114 induce sub-surface ocean warming (≥ 1 °C) in the Nordic Seas^{41,42,67,81–83}. Annual mean sub-surface warming in the Nordic
115 Seas resulting from AMOC weakening, such as that inferred for D–O stadials, is not necessarily simulated in freshwater hosing
116 experiments because of the dominant effect of reduced advection of warm North Atlantic waters into the Nordic Seas and the
117 occurrence of deep-ocean convection⁸⁴ (Fig. 3a). However, as deep-ocean convection occurs in winter close to the sea-ice
118 edge, summer sea-ice melting and increased stratification could lead to sub-surface warming in summer, as inferred from proxy
119 records.

120 As the AMOC leads to northward oceanic meridional heat transport at all latitudes in the Atlantic basin⁸⁵, a weaker AMOC
121 induces warming in the South Atlantic, extending from the surface to intermediate depths, due to weaker ‘heat piracy’^{86–88}
122 (Fig. 2a). Proxy records indeed suggest slightly warmer conditions during D–O stadials than interstadials at mid and high
123 southern latitudes, with a potential southward shift of the thermal subtropical and sub-Antarctic fronts in the South Atlantic^{89–91}
124 and an ~ 1 °C SST increase in the sub-Antarctic and South Pacific^{92–94} (Fig. 2a). High-resolution Antarctic ice-core records,
125 synchronized with Greenland ice cores through atmospheric methane (CH₄) evolution, also suggest that all stadials of the
126 last glacial period were associated with a multi-millennial ~ 1 °C warming in Antarctica^{44,95–97} (Fig. 1g). This north–south
127 asynchrony, termed the thermal bipolar seesaw^{88,98}, was initially described by a thermodynamic model in which AMOC
128 changes modulate the meridional ocean heat transport⁸⁸, increasing the Southern Ocean heat content, decreasing Southern
129 Ocean sea-ice cover and leading to warming over Antarctica owing to ocean heat release.

130 Climate modelling experiments in which the AMOC is artificially weakened and proxy records (including pollen records,
131 speleothems and the geochemical composition of marine and lake sediment) provide evidence for changes in the hydrological
132 cycle during D–O stadials. Lower SSTs in the North Atlantic, coupled to a strengthening of the subtropical high-pressure
133 system in the North Atlantic, lead to drier conditions over southern Europe and the Mediterranean region^{53,64,79,99–102} (Fig.
134 2c). For example, numerical simulations performed with climate models under glacial conditions estimate a reduction in
135 precipitation of approximately -10 cm yr⁻¹ over southern Europe⁷⁹. Stadials were also associated with drier conditions in
136 the northern tropical Atlantic (~ -10 cm yr⁻¹)^{45,79} (Fig. 1e) and wetter conditions in the southern tropical Atlantic ($\sim +10$ cm
137 yr⁻¹)^{69,79}, with a stronger South American monsoon^{103–105} (Fig. 2c). Furthermore, analyses of marine sediment cores and
138 freshwater hosing experiments suggest a weaker Indian summer monsoon during stadials^{45,53,79,106–109}. Although higher $\delta^{18}\text{O}$
139 values recorded in speleothems from China (Fig. 1f) have been interpreted as reflecting a weaker East Asian Monsoon during
140 stadials^{43,110,111}, this is not consistently supported by numerical simulations performed with coupled climate models^{79,107} (Fig.
141 2c). The latitudinal location of maximum precipitation, the Intertropical Convergence Zone (ITCZ), lies at the energy flux
142 equator, the position of which depends on the tropospheric air-temperature difference between the hemispheres¹¹². Cooler
143 conditions over, at least part, of the high northern latitudes and warmer conditions at high southern latitudes thus induce a
144 southward shift of the ITCZ in the Atlantic and Indian Ocean sectors during stadials^{39,53,79,107,108,112}, consistent with the
145 hydrological changes observed in the palaeo records.

146 D–O stadials are therefore characterized by the following climatic changes, consistent with a change in oceanic meridional
147 heat transport in the Atlantic: sea-ice advance in the Nordic Seas; cooling over Greenland (~ -12 °C), the North Atlantic (~ -1.5
148 °C at mid latitudes and ~ -4 °C close to the sea-ice front) and Europe; and small-amplitude (~ 1 °C) warming at mid and high
149 southern latitudes. D–O stadials are also associated with drier conditions in southern Europe and over the northern Tropics,
150 while the southern Tropics become wetter, consistent with a southward shift of the ITCZ. Numerical simulations suggest that
151 the observed climatic and oceanic geochemical changes are consistent with a weaker AMOC.

[H2] Heinrich stadials.

In Greenland ice cores, the amplitude of the $\delta^{18}\text{O}$ and correlated temperature changes that occur during D–O and Heinrich stadials are similar (Fig. 1b), even though Heinrich stadials are usually longer than non-Heinrich stadials^{14,28,44}. Proxy records suggest that sea-ice cover is perennial in the Norwegian Sea and reaches 62°N ^{41,42} during Heinrich stadials and that the cooling in the northern North Atlantic is similar to that during D–O stadials^{20,49,50}. However, additional data are needed to better constrain the full extent of the sea-ice advance in the Nordic Seas and northern North Atlantic during Heinrich stadials. Over southern Europe, the cooling is usually larger during Heinrich stadials than D–O stadials^{62–64}. In marine sediment cores from the western Iberian margin and the Mediterranean Sea, the SST anomalies are twice as large ($\sim 3^\circ\text{C}$) for Heinrich stadials^{26,65,66} (Fig. 1d and Fig. 2a,b).

Heinrich events are characterized by a particularly high IRD abundance in North Atlantic sediments^{20,25,48–51}, indicating sustained iceberg discharge and transport to core sites. In addition, compared with D–O stadials, Heinrich stadials are associated with higher amplitude climatic anomalies in the North Atlantic and far-field regions (as detailed below), thus pointing to a very weak or even fully shutdown AMOC^{15,38,54,113}. Numerical simulations performed with coupled climate models indeed suggest that an AMOC shutdown reduces the meridional oceanic heat transport to the North Atlantic by $\sim 40\%$ ($\sim 0.8\text{ PW}$ at 30°N)^{53,79,114} (Fig. 2b), thus leading to strong North Atlantic cooling ($\sim 3\text{--}6^\circ\text{C}$). As deep-ocean convection brings surface waters that are close to freezing point to depth, reduced deep-water formation in the Nordic Seas leads to sub-surface warming⁸⁴ (Fig. 3). In addition, as deep-water formation in the Nordic Seas weakens, so does transport through the East Greenland current, which brings cold water to the northwestern Atlantic. As a result, the sub-surface temperature increases in the Greenland Sea, the Labrador Sea and in the northwestern Atlantic^{84,115,116}. The geographical location and depth of the sub-surface warming is dependent on changes in the site of deep-water formation and associated changes in sub-surface currents.

Proxies for oceanic circulation provide further support for a very weak AMOC during Heinrich stadials. For example, the sedimentary $^{231}\text{Pa}/^{230}\text{Th}$ in the North Atlantic increases towards the production ratio^{10,68,117} (Fig. 1a), indicating a notable reduction in the southward advection of Pa at depth in the North Atlantic, in agreement with an AMOC shutdown. Furthermore, $\delta^{13}\text{C}$ decreases in the intermediate and deep North Atlantic^{71,72,118–120} (although the signal is muted for Heinrich stadials 2 and 3)^{40,73}, and $[\text{CO}_3^{2-}]$ decreases in the deep South Atlantic, both indicating reduced NADW transport⁷⁶.

Hydrological changes are also generally larger during Heinrich than D–O stadials. Relative to an interstadial, conditions are much drier over southern Europe, the Mediterranean ($\sim 20\text{ cm yr}^{-1}$)^{64,99–102} and the northern tropical Atlantic (~ 20 to -40 cm yr^{-1})^{45,121,122}. The Indian summer monsoon is weaker (~ 20 to -40 cm yr^{-1})^{45,106,108,109,123}, and possibly also the East Asian Monsoon^{43,110,111} (Fig. 1e,f and Fig. 2d). By contrast, wetter conditions prevail in the southern tropical Atlantic ($\sim +10\text{--}30\text{ cm yr}^{-1}$)⁶⁹, and the South American monsoon is stronger^{103–105}. Heinrich stadials have thus been associated with more spatially extensive and more extreme southward shifts of the ITCZ^{39,45,53,112,124–126} (Fig. 2d).

The greater amplitude of the AMOC changes, and the associated changes in oceanic meridional heat transport, during Heinrich stadials leads to more pronounced warming at mid to high southern latitudes (Fig. 2b). Proxy records suggest a southward shift of the thermal subtropical and sub-Antarctic fronts in the South Atlantic^{89–91}, a $2\text{--}3^\circ\text{C}$ ($\pm 0.5^\circ\text{C}$) SST increase in the sub-Antarctic and South Pacific^{92–94}, and a multi-millennial $2\text{--}3^\circ\text{C}$ ($\pm 1^\circ\text{C}$) increase in surface air temperature over Antarctica^{44,95,97} (Fig. 1g).

Freshwater hosing experiments performed with climate models consistently simulate a South Atlantic SST increase, of up to 3°C , as a result of an AMOC cessation^{53,79} (Fig. 2b). However, not all simulations display a SST increase in the South Pacific Ocean, and the magnitude of the simulated temperature increase over Antarctica is lower ($\sim 0.5^\circ\text{C}$) than suggested by proxy records^{53,79,127,128}. The magnitudes of the surface temperature increase over Antarctica and the Southern Ocean are, however, correlated, confirming the important role of ocean processes in Antarctic warming⁷⁹, even if regional differences in the temperature response over Antarctica are most likely due to atmospheric processes¹²⁷. These simulations thus highlight the limits of the bipolar seesaw theory: an AMOC weakening and associated change in meridional oceanic heat transport might not explain the full magnitude of the high-southern-latitude warming. Instead of just passively responding to AMOC changes,

196 changes in Southern Ocean dynamics might need to be invoked^{98,129}. Enhanced deep-ocean convection in the Southern Ocean
197 during stadials^{130,131}, resulting from stronger and/or poleward-shifted Southern Hemisphere westerlies or reduced surface
198 buoyancy, would increase the ocean meridional heat transport towards Antarctica¹³². In turn, this change would lead to surface
199 ocean warming, sea-ice decrease and warmer conditions at high southern latitudes^{132–135}.

200 Even if the response of Southern Hemisphere westerlies to Heinrich stadials is poorly constrained, temperature changes in
201 the North Atlantic could affect the Southern Hemisphere westerlies through an atmospheric tropical bridge^{127,128}. As the ITCZ
202 corresponds to the ascending branch of the Hadley cell, a southward ITCZ shift strengthens the Northern Hemisphere Hadley
203 cell, owing to increased heat transport by the Northern Hemisphere Hadley cell to compensate for reduced northward oceanic
204 heat transport¹³⁶. This strengthening of the Northern Hemisphere Hadley cell in turn weakens the Southern Hemisphere
205 Hadley cell. An associated weakening of the Southern Hemisphere subtropical jet would shift the Southern Hemisphere
206 eddy-driven jet poleward and strengthen the Southern Hemisphere surface westerlies^{137,138}. Although additional constraints on
207 the response of Southern Hemisphere westerlies to North Atlantic cooling are needed, Antarctic ice-core isotopic records¹³⁹
208 indicate a strengthening and poleward shift of the Southern Hemisphere westerlies during stadials. This rapid atmospheric
209 teleconnection between the North Atlantic and the Southern Ocean would be superposed onto a slower oceanic teleconnection.

210 Enhanced deep-ocean convection in the Southern Ocean during Heinrich stadials, potentially resulting from strengthening
211 of the Southern Hemisphere surface westerlies, could explain the observed concurrent increase in CO₂ concentration (Fig. 1h),
212 through increased upwelling of carbon-rich deep waters to the surface^{46,132,134,140,141}. Deep-ocean convection in the Southern
213 Ocean would lead to further sea-ice retreat¹³², which could also contribute to the CO₂ rise¹⁴². Increased dissolved oxygen
214 content and reduced ventilation ages in the deep South Atlantic during Antarctic warm events may corroborate this possibility
215 by pointing to increased Southern Ocean ventilation^{91,130,131}.

216 Palaeoproxy records suggest that the formation of North Pacific Intermediate Water (NPIW) was probably stronger during
217 Heinrich stadial 1 than during either the Last Glacial Maximum (LGM; ~20 ka) or the Holocene^{143–145}. Numerical simulations
218 show that, when the Bering Strait is closed, an AMOC shutdown could enhance NPIW formation^{143,146–148} through a reduction
219 in moisture transport from the Atlantic to the Pacific, coupled to reduced precipitation in the western equatorial Pacific owing to
220 the southward shift of the ITCZ. Increased surface salinity in the Northwest Pacific could then strengthen NPIW formation,
221 which would be reinforced through the Stommel feedback by enhanced advection of low-latitude saline waters. The associated
222 increase in heat transport to the northeast Pacific could lead to warmer and wetter conditions over North America (Fig. 2b),
223 thus potentially affecting the LIS mass balance. In addition, through enhanced ventilation of carbon-rich intermediate North
224 Pacific waters, a stronger NPIW would contribute to a CO₂ increase¹⁴⁹.

225 The climatic imprint of Heinrich stadials is thus similar to that of D–O stadials, but they are longer, and the amplitude
226 of the climatic and oceanic geochemical changes is generally larger, consistent with a weaker AMOC (Fig. 4). A weaker
227 AMOC is also consistent with larger changes in Northern Hemisphere ice sheets and iceberg discharges into the North Atlantic
228 during Heinrich stadials. The larger high-southern-latitude warming and considerable CO₂ increase occurring during Heinrich
229 stadials further point to changes in Southern Ocean processes, potentially linked to a non-linear or threshold response to AMOC
230 changes.

231 [H2] *Interstadials.*

232 Temperature reconstructions from the North Greenland Ice Core Project (NGRIP) suggest that D–O events of the last glacial
233 period are characterized by a mean temperature increase of 12 ± 2.6 °C over a few decades¹⁴. Each episode of abrupt Greenland
234 warming during MIS 3 was associated with a reduction in Norwegian Sea sea-ice cover, the spring sea-ice edge shifting north
235 of ~62°N^{41,42} and an abrupt 4–6 °C increase in North Atlantic summer SST^{49,50}.

236 This rapid North Atlantic temperature increase and sea-ice reduction is most likely due to the resumption of deep-ocean
237 convection and thus NADW formation in the Nordic Seas^{38,39,42,48,67,82,150}. Evidence for a consistently strong AMOC during
238 interstadials also comes from low North Atlantic sedimentary ²³¹Pa/²³⁰Th^{10,68,117} (Fig. 1a), the magnetic properties of North
239 Atlantic sediment¹⁵¹ and a high [CO₃²⁻] in the deep sub-Antarctic Atlantic Ocean⁷⁶.

240 A strong AMOC, similar to today's, is also consistent with the relatively warm and wet conditions over Europe and the
241 Mediterranean region recorded during each interstadial^{28,63,64,99–102,152–154}. In addition, Greenland and Antarctic ice-core
242 records indicate that changes in the concentration of atmospheric CH₄ are tightly coupled to D–O variability^{155–157}. As the
243 dominant source of CH₄ to the atmosphere is anaerobic decomposition of organic matter in low-latitude wetlands¹⁵⁸, CH₄
244 variations indicate changes in the hydrological cycle of tropical and subtropical regions¹⁵⁵. As northern tropical wetlands cover
245 a larger area than their southern counterparts, the relatively high atmospheric CH₄ concentration recorded in high-resolution
246 Antarctic ice cores during all interstadials of the last glacial period¹⁵⁹ (Fig. 1c) suggests a northward position of the ITCZ¹⁶⁰,
247 consistent with a strong AMOC¹¹².

248 To summarize, palaeoproxy records from the Atlantic basin indicate changes in oceanic circulation associated with D–O
249 cycles of the last glacial period. In addition, there is substantial evidence for concurrent climatic variations in both proximal and
250 distal regions, including southern high latitudes, which are consistent with AMOC changes. Together, the available observational
251 records and numerical experiments indicate AMOC weakening during the transition to a D–O stadial, further AMOC weakening,
252 or even shutdown, during Heinrich stadials and rapid AMOC strengthening towards interstadial conditions^{10,38,39,117} (Fig. 4).
253 However, what led to these AMOC variations?

254 [H1] Processes involved in D–O variability

255 Although the expression of D–O variability is relatively well constrained (except for details in relative phasing), particularly
256 in the Atlantic region, and there is substantial evidence for its association with AMOC changes, the processes leading to this
257 variability are still highly debated. No hypothesis can explain all inferred climate changes of the D–O and Heinrich continuum,
258 raising questions regarding their origin. We address these questions in this section. Specifically, we consider whether the
259 variability is internal to the atmosphere–ocean–sea-ice system^{55–58} and whether changes in *p*CO₂ could trigger the transitions⁶⁰.
260 Moreover, we discuss whether ice-sheet discharges are needed to explain non-Heinrich stadials, and whether the correspondence
261 of Heinrich events with D–O stadials represents the phase locking of two separate oscillatory systems through, for example,
262 stochastic resonance^{161–163}. We also address questions regarding the processes involved in Heinrich events and the role of
263 background conditions in AMOC stability.

264 [H2] *Internal oscillations.*

265 Early studies hypothesized that D–O cycles were the result of a ‘salt oscillator’^{54,113}, whereby warm and wet conditions in
266 the Northern Hemisphere during interstadials, associated with increased continental ice-sheet melt, result in greater surface
267 buoyancy in the North Atlantic, thus weakening NADW formation and the AMOC. Cold and dry conditions in the Northern
268 Hemisphere during stadials, due to the southward shift of the ITCZ, would increase salinity in the tropical North Atlantic thus
269 strengthening the AMOC^{164,165} (Fig. 5). Numerical experiments^{55,57,164} and palaeoproxy records^{67,81} provide support for
270 the role of a North Atlantic salt oscillator during D–O cycles, highlighting the tight coupling between sea ice, North Atlantic
271 salinity transport and NADW formation.

272 Internal millennial-scale AMOC variations have been simulated in coupled climate models^{55–58,166–168}, usually under
273 specific boundary conditions. Some of these oscillations were initiated by stochastic atmospheric forcing^{167,168} or stochastic
274 changes in the Nordic Seas overturning circulation¹⁶⁶. In other models, the radiative balance led to sea-ice growth, and the
275 associated North Atlantic salinity re-distribution was sufficient to induce fairly rapid (≤ 500 years) cooling towards stadial
276 conditions^{55,57}. The interstadial transition is then initiated by a reorganization of the vertical thermohaline structure of the
277 northern North Atlantic. On the basis of palaeoproxy records^{42,67,81,82}, it has been postulated that extensive perennial sea-ice
278 cover and a strong halocline in the Nordic Seas during stadials would prevent heat transfer to the atmosphere and lead to an
279 increase in heat content below the pycnocline (a depth of ~ 300 m; Figs 3 and 5). Although a simple column model of the
280 Nordic Seas has shown that this heat build-up below the pycnocline could induce convective overturning¹⁶⁹, the convective
281 overturning in coupled models occurred in the northern North Atlantic owing to either a northward salinity flux below the

282 sea-ice lid⁵⁵ or the creation of a super polynya⁵⁷. However, these simulated convective overturning events were obtained by
283 adjusting the diapycnal diffusivity profiles of the ocean models^{55,57}. Additional work is thus required to assess whether such
284 convective overturning events could arise in the Nordic Seas under intermediate glacial conditions.

285 The cooling towards stadial conditions would potentially be slower, and thus in better agreement with palaeo records, if it
286 involved the build-up of extensive ice shelves in the Labrador and/or Nordic Seas^{170,171}. There is some observational support
287 for the presence of fringing ice shelves around Greenland during the last glacial interval^{172,173}. However, the current evidence
288 suggests that Baffin Bay was not covered by a full ice shelf at the LGM and, thereby, perhaps also during MIS 3¹⁷⁴.

289 An outstanding challenge for models is to obtain D–O-like oscillations under only appropriate boundary conditions and
290 forcings. Oscillatory behaviour under fixed boundary conditions has been observed in only a few modelling experiments^{55–58},
291 some of which used very specific boundary conditions, including pre-industrial Northern Hemisphere ice sheets, low obliquity
292 (22°), low CO₂ concentration (≤ 217 ppm)^{56,58,166} or LGM boundary conditions^{55,57}, that do not match those of MIS 3 when
293 D–O variability was most prevalent.

294 [H2] *Impact of atmospheric CO₂ changes on the AMOC.*

295 Heinrich stadials are associated with an increase in CO₂ concentration of up to ~20 ppm, followed by a millennial-scale
296 20–30 ppm decrease^{46,141} (Fig. 1h). However, current records are unable to resolve significant CO₂ concentration changes
297 during D–O stadials, and MIS 3 includes multi-millennial periods with D–O events but CO₂ changes of <10 ppm. A gradual
298 CO₂ increase could lead to abrupt AMOC strengthening at the end of Heinrich stadials by decreasing the sea-ice cover in the
299 North Atlantic either directly or through increased salt transport from the tropical to the North Atlantic^{59,60,175}. This AMOC
300 sensitivity to CO₂ changes seems to occur in models that display deep-water formation in the northern North Atlantic, south of
301 Iceland. By contrast, models that simulate deep-water formation in the Nordic Seas display a much higher AMOC stability to
302 changes in CO₂ under MIS 3 boundary conditions¹⁷⁶, potentially indicating that AMOC stability is dependent on the location
303 and strength of deep-water formation.

304 [H2] *Meltwater discharges and D–O stadials.*

305 $\delta^{18}\text{O}$ records from the Norwegian and Irminger Seas are consistent with decreases in sea-surface salinity (and thus halocline
306 strengthening) occurring in phase with stadials^{49,81}, possibly due to melting and calving of the circum-North Atlantic ice
307 sheets^{177,178}. It is, however, unclear whether the magnitude of the associated meltwater input would have been sufficient to
308 weaken the AMOC. Although the AMOC stability generally seems to be lower under intermediate glacial conditions than
309 interglacial ones^{38,39,60,179}, only a few models are very close to the stability threshold^{60,179}. However, changes in LIS height
310 could have also directly affected the AMOC strength through changes in North Atlantic windstress, thus lowering the stability
311 threshold^{59,60}.

312 Calving of circum-North Atlantic ice sheets is supported by the presence of IRD layers in North Atlantic marine sediment
313 cores during all D–O stadials^{20,47,51}. Iceberg discharges require a marine ice-sheet boundary. The cold surface air and SSTs
314 during stadials would have promoted marine ice-sheet expansion¹⁷⁷. But with the stadial accumulation of heat below the
315 halocline, these marine margins could have then become destabilized with a resultant increase in iceberg discharges¹⁷⁸. A
316 complication for causal inference is that the presence of IRD also reflects, to an uncertain extent, enhanced preservation of
317 icebergs owing to colder near-surface ocean temperatures as they are advected to the marine core sites. Therefore, it has
318 also been suggested that North Atlantic cooling preceded IRD deposition, thus implying that iceberg discharges could be a
319 consequence and not a cause of stadials²⁰.

320 Although Nordic Seas sea ice, freshwater balance and thus stratification appear to have a key role in D–O variability,
321 further work is needed to fully understand the underlying processes. In this regard, key questions to resolve are: what are the
322 mechanisms involved specifically in Heinrich events, and how do they relate to D–O cycles?

323 [H2] *Processes leading to Heinrich events.*

324 From the mid-Pleistocene transition (~640 ka), Heinrich events are identified by thick layers of IRD originating from the
325 Hudson Strait, thus indicating LIS discharges. Red Sea isotope records and fossil coral data suggest that Heinrich events could
326 have been associated with a global mean sea-level rise of >15 m (refs^{36, 180–182}). However, the amplitude and, especially, the
327 timing of these potential sea-level variations are still uncertain¹⁸³. Given the evidence for Hudson Strait provenance of IRD and
328 substantial sea-level change, LIS dynamics have been proposed to explain Heinrich events¹⁷⁷.

329 The most prominent theories include a growth–purge mechanism (usually referred to as binge–purge), which involves
330 free oscillations of the ice stream owing to build-up and subsequent purging of basal ice at the pressure melting point for
331 ice streaming¹⁸⁴. A numerical simulation performed with a coupled ice-sheet and simplified climate model¹⁸⁵ obtained
332 multi-millennial oscillations with an associated change in LIS ice volume equivalent to a sea-level change of 5–10 m. For this
333 model, each Heinrich event was triggered by small-scale instabilities of the ice sheet at the mouth of the Hudson Strait. In
334 addition, a comparison of ice-sheet models¹⁸⁶ found the growth–purge mechanism to be fairly robust across most participating
335 models, with a strong dependence of ice-loss magnitude on the parameterization of the basal sliding rate and with periods in the
336 5–17 kyr range, depending on the model. This study also showed that the oscillations cease with higher temperatures owing to
337 sustained ice streaming.

338 Complementary theories have sought to more directly link LIS disintegration to climatic conditions or to elucidate the
339 physical trigger mechanism that was idealized in previous studies¹⁸⁵. Sub-surface warming in the northern North Atlantic
340 and Nordic Seas during AMOC weakening^{67, 81, 115, 187, 188} could trigger iceberg discharges in the Hudson Strait through two
341 mechanisms: the break-up of an ice shelf on the Labrador Sea, or direct retreat of marine-terminated LIS. The first mechanism
342 assumes that stadial conditions would enable the formation of a large ice shelf at the mouth of the Hudson Strait, in part
343 through buttressing and the suppression of submarine convection by adjacent sea ice¹⁸⁹, especially land-fast ice¹⁹⁰. This ice
344 shelf would be vulnerable to intra-stadial climate ameliorations^{172, 174} and/or sub-surface warming resulting from a weaker
345 AMOC^{115, 187, 191, 192}, thus inducing catastrophic ice-shelf break-up and a loss of buttressing of the Hudson Strait ice stream.
346 To date, however, it is unclear whether a substantial ice shelf developed at the mouth of the Hudson Strait during glacial
347 times. Even without the presence of a large terminal ice shelf, the Hudson Strait ice stream was marine terminating and
348 thus subject to potentially high melt from sub-surface ocean warming, which could facilitate fast marine margin retreat. If
349 such a sub-surface warming also extended into the Greenland and Nordic Seas, and at a depth where it could affect the
350 marine-terminated ice sheets or ice shelves, as inferred from some climate model experiments^{84, 115, 135, 188} (Fig. 3), then it
351 could lead to concurrent discharges of the European and Greenland ice sheets^{178, 193}. Isostatic adjustment of the sill elevation
352 at the mouth of the Hudson Strait could also control the contact between warm sub-surface waters and the calving face and,
353 thus, modulate LIS discharges¹⁹⁴. These hypotheses can therefore explain the occurrence of Heinrich events during stadials²⁰,
354 as well as the occurrence of simultaneous disintegration events from other circum-Atlantic ice sheets through sub-surface
355 warming. However, although there is some observational evidence for sub-surface warming of the Norwegian Sea^{67, 81, 82} and
356 northwestern Atlantic¹¹⁵ during Heinrich stadials, additional studies are needed to constrain the magnitude, location and depth
357 of this warming.

358 Changes in the southern extent or height of the LIS could also directly affect North Atlantic sea-ice concentration,
359 temperature^{195–197} and the AMOC⁵⁹ by modulating the strength and position of the North Atlantic westerlies. There is some
360 evidence for a dynamic LIS during MIS 3: radiocarbon dates and relative sea-level constraints are consistent with a LIS
361 southern margin proximal to the southern edge of Hudson Bay (~51°N) during the interstadial at 46.7 ka, followed by a fast
362 southward advance to ~44°N during Heinrich stadial 4 and subsequent retreat¹⁹⁸. Thus, a dynamic LIS may have modulated the
363 AMOC strength, either through atmospheric steering or freshwater delivery to the North Atlantic (as the southern extent would
364 determine whether central LIS meltwater was routed southward to the Gulf of Mexico or eastward to the North Atlantic)¹⁹⁹.

[H2] Background conditions and AMOC stability.

Although D–O variability *stricto sensu* is suppressed during interglacial times owing to the lack of large circum-Atlantic ice-sheets, recent palaeoproxy records have highlighted periods of weaker AMOC during several interglacial periods^{200–202}. The processes leading to these AMOC weakenings are poorly constrained, but some of these weakenings could be due to meltwater discharges from the Greenland ice sheet²⁰³. Nevertheless, during interglacial times, the AMOC seems to be in a relatively stable strong state, and the AMOC perturbations are of lower magnitude than those during glacial periods.

The prevalence of D–O variability during intermediate glacials indicates that background conditions, including CO₂ concentration, the size of Northern Hemisphere continental ice sheets and the associated sea level most likely influence the AMOC stability. Owing to the presence of Northern Hemisphere ice sheets, colder conditions in the North Atlantic and larger sea-ice coverage under glacial conditions, the AMOC transition threshold during intermediate glacial states seems to be lower than during interglacials — that is, a smaller perturbation is needed to significantly increase the sea-ice coverage and weaken the AMOC^{38, 39, 179, 204}. The closure of the Bering Strait, with its shallow sill depth at ~50 m below sea level, further lowers the perturbation threshold²⁰⁵ owing to its influence on the North Atlantic freshwater budget. On the one hand, the closure of the Bering Strait strengthens the AMOC by hampering the flow of low-salinity Pacific waters towards the Arctic^{205, 206}. On the other hand, when the Bering Strait is closed, freshwater pulses would lead to persistent low-salinity anomalies in the North Atlantic, as they cannot be flushed out through the Bering Strait²⁰⁷. In addition, numerical experiments suggest that the formation of NPIW could strengthen when the AMOC weakens considerably and the Bering Strait is closed^{143, 146}. This change in the NPIW could lead to warmer and wetter conditions over North America²⁰⁸ (Fig. 5) and thus affect the LIS mass balance.

Using a zonally averaged multibasin model, it was suggested that a weak (stadial) AMOC state with deep convection south of Iceland could be stable under glacial conditions³⁸. However, modelling studies performed with coupled climate models under intermediate glacial background conditions found the AMOC to be bi-stable, shifting between a weak and strong state following small perturbations to the system^{59, 60, 179}, or with a stable strong AMOC state¹⁷⁶ and temporarily stable AMOC off state following meltwater perturbations³⁹. It is thus likely that both the stability of the AMOC is lower and the perturbations to the system are greater during intermediate glacial than interglacial states owing to the presence of larger Northern Hemisphere ice sheets. As developed further below, perturbations to the system are not restricted to meltwater input, but also include centennial-scale changes in Northern Hemisphere ice sheets, CO₂ concentration and sub-surface warming.

Finally, palaeoproxy records suggest that the AMOC was shallower^{209, 210} and potentially weaker^{211–213} during the LGM, whereas most of the Paleoclimate Modelling Intercomparison Project phase 3 and 4 (PMIP3 and PMIP4) LGM experiments suggest the AMOC was as strong as during interglacials^{214, 215}. This discrepancy between the AMOC state inferred from proxy records and modelling suggests that either the glacial perturbations (in this case, most likely meltwater input) are poorly constrained or that deep-water formation does not occur at the ‘right place’ in the models, making them overly sensitive to changes in North Atlantic windstress. Through strengthening of the North Atlantic windstress, a large LIS could lead to a strong AMOC²¹⁶, which would likely be more stable and less prone to internal oscillations^{38, 56, 58, 176}. Strong westerly windstress over the North Atlantic indeed strengthens the subpolar gyre, the salt transport in the Irminger current and the eddy salt flux to the centre of the gyre, which would favour NADW formation^{217, 218}. However, the importance of this process is likely dependent on the location of deep-water formation (that is, in the Labrador or Nordic Seas). Indeed, in contrast to recent estimates¹, in some historical CMIP5 simulations, deep water primarily formed in the Labrador Sea²¹⁹.

[H1] Synthesis and proposed oscillatory system

Although a complete explanation for D–O variability remains elusive, a tentative scheme can be advanced. As there is strong coupling between sea-ice formation, deep-ocean convection in the Nordic Seas and the AMOC, a small perturbation in the heat or salt flux in the Nordic Seas, such as increased meltwater runoff from circum-Atlantic ice-sheets, a decrease in CO₂ or other climatic instabilities could lead to sea-ice advance²²⁰, a southward shift of the convection site²²¹ and AMOC weakening, thus leading to a stadial (Fig. 5b).

408 AMOC weakening would reduce the transport of cold surface and sub-surface waters through the Denmark overflow^{1,116}.
409 This change in oceanic circulation, associated with increased sea-ice cover, would lead to sub-surface warming in the Nordic
410 Seas^{81,135} and the Northwestern Atlantic^{115,188} (Fig. 3). In turn, Northwestern Atlantic sub-surface warming could have
411 triggered the disintegration of a Labrador Sea ice shelf^{115,191} or the retreat of the Hudson Strait ice stream¹⁹⁴, thus leading to the
412 Hudson Strait iceberg discharges characteristic of Heinrich events. Recurrent episodes of AMOC weakening and sub-surface
413 warming would trigger a Heinrich event only when ice-shelf or ice-sheet conditions permitted (depending on, for example,
414 ice-sheet thickness and basal ice temperature), thus providing a plausible explanation for the link between D–O cyclicity and
415 Heinrich events.

416 Further AMOC weakening during a Heinrich stadial is linked to sea-ice advance and the lack of sustained deep-ocean
417 convection. The transition to an interstadial would arise from an increase in surface salinity in the northern North Atlantic
418 and/or a decrease in sea-ice extent. The proposed mechanisms are not mutually exclusive and include convective overturning in
419 the Nordic Seas, brought about by the sub-surface warming⁸¹; increased transport of low-latitude salty surface waters to the
420 North Atlantic¹⁶⁴, potentially amplified by a strengthening of the westerlies over the North Atlantic owing to an increase in LIS
421 height; and/or a gradual CO₂ increase^{59,60} (Fig. 5a). Finally, Southern Ocean processes could also contribute to reinvigoration
422 of the AMOC. Through enhanced Southern Ocean upwelling and Ekman transport of Southern Ocean waters to the Atlantic,
423 a strengthening of Southern Hemisphere westerlies (due to a southward shift of the ITCZ) during Heinrich stadials could
424 strengthen the AMOC by up to 4 Sv (refs^{222,223}). However, eddy compensation in the Southern Ocean could substantially
425 reduce the impact of Southern Hemisphere winds on the AMOC²²⁴. A bipolar ocean seesaw, NADW–Antarctic Bottom Water
426 (AABW), could also strengthen NADW formation after episodes of deep-ocean convection in the Southern Ocean during
427 Heinrich stadials, owing to density differences between NADW and AABW^{225,226}.

428 **[H2] A self-sustained oscillatory framework.**

429 On the basis of the evidence for a 1–2 kyr periodicity of D–O cycles^{23,31,35,49,227,228}, the occurrence of stochastic resonance,
430 both ‘autonomous’ (purely internal to the ocean–sea-ice–atmosphere system) and ‘non-autonomous’ (arising from the influence
431 of an external, possibly periodic, forcing), has been proposed^{161–163}. However, the numerical models first used to investigate
432 the role of stochastic resonance in D–O variability were box models, lacking important processes and feedbacks. As detailed
433 above, improvements in climate modelling capacity as well as additional and more detailed palaeorecords now provide a clearer
434 picture of the processes at play.

435 We thus propose that the D–O variability could be explained by a self-sustained oscillatory framework of the coupled
436 climate–ice-sheet system, which would be characterized by a relatively low stability of the AMOC in its strong state under
437 intermediate glacial conditions. Small perturbations (for example, centennial-scale changes in the northern North Atlantic
438 freshwater balance, CO₂ or wind) could then lead to AMOC weakening and an associated rapid Northern Hemisphere sea-ice
439 advance into a stadial. This AMOC weakening and sea-ice advance would induce climatic changes, including sub-surface
440 warming in the northern North Atlantic and a southward shift of the ITCZ, with the latter leading to saltier conditions in the
441 tropical North Atlantic. On a multi-centennial timescale, these climatic changes act as negative feedback on the AMOC and
442 sea-ice changes, thus leading to AMOC recovery and rapid sea-ice retreat into an interstadial. Depending on the state of the
443 LIS, and possibly the surrounding ice shelves, the initial AMOC weakening and associated climatic changes could trigger
444 the LIS discharges characteristic of Heinrich events, which act as a positive feedback, amplifying the AMOC weakening and
445 sea-ice advance. An AMOC off state, with enhanced NPIW and AABW formation, could then be marginally stable. However,
446 the larger amplitude of the anomalies generated during Heinrich stadials, particularly North Atlantic sub-surface warming,
447 changes in LIS extent, strengthening of Southern Hemisphere westerlies and CO₂ increase, would have the potential to trigger
448 AMOC recovery and even overshoot (Figs. 1 and 5). Such an AMOC overshoot and associated North Atlantic surface warming
449 could then push the system back towards stadial conditions.

450 From this synthesis of the proposed D–O sequence tentatively emerges an oscillatory system characterized by self-sustained
451 centennial to millennial scale variations in the ocean–sea-ice–atmosphere system that resonate with (and help to trigger)

452 multi-millennial scale variations in marine-based ice sheets, potentially through ice-shelf-related dynamical instabilities. The
453 expression of this oscillatory system would, in theory, be amplified or damped (turned on or off) according to the background
454 climate state (for example, temperature, salinity and wind stress), which is also linked to ice volume. The preponderance of
455 D–O variability during intermediate glacial states indeed suggests a dependence on background conditions, including any or all
456 of the following: the presence of the LIS, but of moderate size so as not to induce strong North Atlantic westerly windstress,
457 such as prevails at the LGM^{214,216}; relatively high boreal summer insolation at high northern latitudes, leading to summer melt
458 of circum-Atlantic ice-sheets; and sea-level modulation (if not closure) of the Bering Strait throughflow, which would affect the
459 North Atlantic freshwater budget and AMOC stability^{205,206}. However, it should be noted that D–O cycles 4 and 3 occurred
460 when the LIS was large and the summer insolation at high northern latitudes was moderate.

461 [H1] Summary and outlook

462 Glacial periods of the Pleistocene, and particularly glacial states with an intermediate Northern Hemisphere ice-sheet volume,
463 are characterized by millennial-scale climate variability^{23,25–27,31,33}. This D–O variability involves variations in AMOC
464 strength and Nordic Seas sea ice, thus leading to surface temperature changes of opposite signs and asynchronous timing in
465 both hemispheres²². The climatic expression of D–O variability is fairly well constrained in the Atlantic region and surrounding
466 landmasses, but the knowledge of its expression in other regions is more limited owing to a lack of high-resolution proxy records,
467 issues with age constraints and interpretations, as well as a lack of knowledge on the oceanic and atmospheric teleconnections
468 arising from a weaker AMOC and associated cooler North Atlantic.

469 The sequence of events that led to D–O climatic variability is still highly debated. Several mechanisms have been put
470 forward to explain the D–O variability; however, none can currently replicate all the characteristics of D–O cycles, including
471 their preponderance during intermediate glacial states. Here, we propose a self-sustained oscillatory model of the climate–
472 ice-sheet system, modulated by background climatic conditions, to synthesize observations and current understanding of the
473 underlying processes. In this self-sustained oscillatory conceptual framework centred on AMOC and Nordic Seas sea-ice
474 changes, which feed back on each other, the climatic, CO₂ and ice-sheet changes occurring during stadials provide a negative
475 feedback on the AMOC and Nordic Seas sea-ice cover, thus leading to the AMOC reinvigoration to interstadial conditions (Fig.
476 5b), and vice versa. D–O variability would not be a simple response to meltwater fluxes. Instead, D–O cyclicity would represent
477 an emergent phenomenon rooted in the ocean–sea-ice–atmosphere system and linked to ice-sheet dynamics (and therefore
478 Heinrich events) through the impact of AMOC changes on ice-shelf stability and/or ice streaming, as well as through potential
479 positive feedbacks from meltwater delivery on AMOC strength. This framework complements the previously suggested AMOC
480 hystereses as a function of meltwater input⁸, LIS or CO₂ changes^{59,60} as it acknowledges that the AMOC does not only respond
481 to but also influences the climate, ice sheets and the carbon cycle.

482 The principal challenge in further developing these theories is that current Earth system models do not include all necessary
483 components (for example, biogeochemistry, ice shelves, ice-sheet dynamics), inadequately represent important processes
484 or cannot be integrated long enough under intermediate glacial conditions to simulate self-sustained D–O cycles. NADW
485 formation in climate models is highly parametrized and not well constrained by observations, so there is little confidence in
486 simulated changes in the strength and location of NADW formation in response to climate change, both past and future. Owing
487 to relatively long integration times necessary to understand the processes involved in D–O variability, numerical experiments
488 have been performed with simpler or relatively coarse resolution climate models that do not include ice sheets and/or do not
489 adequately resolve relevant boundary currents and key marine sills. Given the complexity of the oceanic circulation in the
490 North Atlantic and Nordic Seas regions, and the central role of mesoscale eddies in salt and heat transport, the processes at play
491 could be better constrained by performing numerical experiments with higher-resolution coupled climate models. Coupled
492 climate–ice-sheet model simulations of past glacial periods are starting to emerge¹⁹⁷ but need to be expanded to help in the
493 understanding of the interaction between ice-sheet, ice-shelf, sea-ice and AMOC variations. Additional observational data on
494 the magnitude and timing of glacioeustatic changes in sea levels and Northern Hemisphere ice sheets, and their relative timing

495 with respect to D–O variability, are needed to better constrain the role of changes in ice-sheet volume and associated meltwater
496 input into the ocean. Owing to the strong coupling between sea-ice and deep-water formation, additional records of past
497 millennial-scale changes in sea-ice cover in the Nordic Seas and northern North Atlantic are required. Finally, as sub-surface
498 warming in the northern North Atlantic during stadials likely had an important role in triggering D–O and Heinrich events,
499 additional ocean interior temperature records and process studies are needed to quantify the magnitude, location and depth of
500 this potential warming.

501 Past AMOC changes suggest that the AMOC might be less stable than currently simulated by climate models and/or
502 that the range of processes affecting the buoyancy and dynamics of the North Atlantic and Nordic Seas might be larger than
503 classically thought. As anthropogenic emissions of carbon accumulate in the atmosphere, runoff from the Greenland ice
504 sheet will increase and the Arctic sea-ice extent will continue to decline. These factors are likely to weaken the AMOC, with
505 important implications for the climate, cryosphere and global carbon cycle.

506 References

- 507 1. Lozier, M. S. *et al.* A sea change in our view of overturning in the subpolar north atlantic. *Science* **363**, 516–521 (2019).
- 508 2. Rahmstorf, S. *et al.* Exceptional twentieth-century slowdown in Atlantic Ocean overturning circulation. *Nat. Clim Chang.*
509 **5**, 475–480 (2015).
- 510 3. Marchitto, T. M. & deMenocal, P. B. Late Holocene variability of upper North Atlantic Deep Water temperature and
511 salinity. *Geochem. Geophys. Geosystems* **4**, [10.1029/2003GC000598](https://doi.org/10.1029/2003GC000598) (2003).
- 512 4. Thornalley, D. *et al.* Anomalously weak Labrador Sea convection and Atlantic overturning during the past 150 years.
513 *Nature* **556**, 227–230 (2018).
- 514 5. Kobashi, T. *et al.* Volcanic influence on centennial to millennial Holocene Greenland temperature change. *Sci. Reports* **7**,
515 1441 (2017).
- 516 6. Stommel, H. Thermohaline convection with two stable regimes of flow. *Tellus* **13**, 224–230 (1961).
- 517 7. Reintges, A., Martin, T., Latif, M. & Keenlyside, N. S. Uncertainty in twenty-first century projections of the atlantic
518 meridional overturning circulation in cmip3 and cmip5 models. *Clim. Dyn.* **49**, 1495–1511 (2017).
- 519 8. Hofmann, M. & Rahmstorf, S. On the stability of the Atlantic meridional overturning circulation. *Proc. Natl Acad.*
520 *Sci.USA* **106**, 20584–20589 (2009).
- 521 9. Valdes, P. Built for stability. *Nat. Geosci.* **4**, 414–416 (2011).
- 522 10. Henry, L. *et al.* North Atlantic ocean circulation and abrupt climate change during the last glaciation. *Science* **353**,
523 470–474 (2016).
- 524 11. Dansgaard, W. *et al.* A new Greenland Deep Ice Core. *Science* **218**, 1273–1277 (1982).
- 525 12. Dansgaard, W., Johnsen, S. & Clausen, H. Evidence for general instability of past climate from a 250-kyr ice-core record.
526 *Nature* **364**, 218–220 (1993).
- 527 13. North Greenland Ice Core project members. High-resolution record of Northern Hemisphere climate extending into the
528 last interglacial period. *Nature* **431**, 147–151 (2004).
529 **Presents a highly resolved record of D–O variability in a Greenland ice core.**
- 530 14. Kindler, P. *et al.* Temperature reconstruction from 10 to 120 kyr b2k from the NGRIP ice core. *Clim. Past* **10**, 887–902
531 (2014).
- 532 15. Heinrich, H. Origin and consequences of cyclic ice rafting in the northeast Atlantic Ocean during the past 130,000 years.
533 *Quat. Res.* **29**, 142–152 (1988).

- 534 **16.** Bond, G., Heinrich, H., Broecker, W. & Labeyrie, L. Evidence of massive discharges of icebergs into the North Atlantic
535 during the last glacial period. *Nature* **360**, 245–249 (1992).
- 536 **17.** Bond, G. Correlations between climate records from North Atlantic sediments and Greenland ice. *Nature* **365**, 143–147
537 (1993).
- 538 **Highlights D–O oscillations in marine sediment cores from the North Atlantic and establishes a link to variations**
539 **in Greenland ice-core $\delta^{18}\text{O}$ records.**
- 540 **18.** Hemming, S. Heinrich events: Massive late Pleistocene detritus layers of the North Atlantic and their global climate
541 imprint. *Rev. Geophys.* **42**, 2003RG000128 (2004).
- 542 **19.** Sánchez-Goñi, M. & Harrison, S. Millennial-scale climate variability and vegetation changes during the Last Glacial:
543 Concepts and terminology. *Quat. Sci. Rev.* **29**, 2823–2827 (2010).
- 544 **20.** Barker, S. *et al.* Icebergs not the trigger for North Atlantic cold events. *Nature* **520**, 333–336 (2015).
- 545 **21.** Naafs, B., Hefter, J. & Stein, R. Millennial-scale ice rafting events and Hudson Strait Heinrich(-like) Events during the
546 late Pliocene and Pleistocene: a review. *Quat. Sci. Rev.* **80**, 1 – 28 (2013).
- 547 **22.** Barker, S. *et al.* 800,000 Years of Abrupt Climate Variability. *Science* **334**, 347–351 (2011).
- 548 **23.** Oppo, D. W., McManus, J. F. & Cullen, J. L. Abrupt Climate Events 500,000 to 340,000 Years Ago: Evidence from
549 Subpolar North Atlantic Sediments. *Science* **279**, 1335–1338 (1998).
- 550 **24.** Raymo, M., Ganley, K., Carter, S., Oppo, D. & McManus, J. Millennial-scale climate instability during the early
551 Pleistocene epoch. *Nature* **392**, 699–702 (1998).
- 552 **25.** McManus, J. F., Oppo, D. W. & Cullen, J. L. A 0.5-Million-Year Record of Millennial-Scale Climate Variability in the
553 North Atlantic. *Science* **283**, 971–975 (1999).
- 554 **Provides evidence for millennial-scale climatic variability in the North Atlantic over the past 500,000 years and,**
555 **particularly, during intermediate glacial states.**
- 556 **26.** Martrat, B. *et al.* Four climate cycles of recurring deep and surface water destabilizations on the Iberian margin. *Science*
557 **317**, 502–507 (2007).
- 558 **27.** Hodell, D. A., Channell, J. E. T., Curtis, J. H., Romero, O. E. & Röhl, U. Onset of "Hudson Strait" Heinrich events in the
559 eastern North Atlantic at the end of the middle Pleistocene transition (640 ka)? *Paleoceanography* **23** (2008).
- 560 **28.** Margari, V. *et al.* The nature of millennial-scale climate variability during the past two glacial periods. *Nat. Geosci.* **3**,
561 127–131 (2010).
- 562 **29.** Bailey, I. *et al.* Flux and provenance of ice-rafted debris in the earliest Pleistocene sub-polar North Atlantic Ocean
563 comparable to the last glacial maximum. *Earth Planet. Sci. Lett.* **341-344**, 222 – 233 (2012).
- 564 **30.** Obrochta, S. P. *et al.* Climate variability and ice-sheet dynamics during the last three glaciations. *Earth Planet. Sci. Lett.*
565 **406**, 198 – 212 (2014).
- 566 **31.** Birner, B., Hodell, D. A., Tzedakis, P. C. & Skinner, L. C. Similar millennial climate variability on the Iberian margin
567 during two early Pleistocene glacials and MIS 3. *Paleoceanography* **31**, 203–217 (2016).
- 568 **32.** Hodell, D. A. & Channell, J. E. T. Mode transitions in Northern Hemisphere glaciation: co-evolution of millennial and
569 orbital variability in Quaternary climate. *Clim. Past* **12**, 1805–1828 (2016).
- 570 **33.** Rodrigues, T. *et al.* A 1-Ma record of sea surface temperature and extreme cooling events in the North Atlantic: A
571 perspective from the Iberian Margin. *Quat. Sci. Rev.* **172**, 118 – 130 (2017).
- 572 **34.** Shackleton, N. Oxygen isotopes, ice volume and sea level. *Quat. Sci. Rev.* **6**, 183 – 190 (1987).

- 573 35. Schulz, M., Berger, W., Sarnthein, M. & Grootes, P. Amplitude variations of 1470-year climate oscillations during the
574 last 100,000 years linked to fluctuations of continental ice mass. *Geophys. Res. Lett.* **22**, 3385–3388 (1999).
- 575 36. Siddall, M., Rohling, E. J., Thompson, W. G. & Waelbroeck, C. Marine isotope stage 3 sea level fluctuations: Data
576 synthesis and new outlook. *Rev. Geophys.* **46**, [10.1029/2007RG000226](https://doi.org/10.1029/2007RG000226) (2008).
- 577 37. Kawamura, K. *et al.* State dependence of climatic instability over the past 720,000 years from Antarctic ice cores and
578 climate modeling. *Sci. Adv.* **3**, e1600446 (2017).
- 579 38. Ganopolski, A. & Rahmstorf, S. Rapid changes of glacial climate simulated in a coupled climate model. *Nature* **409**,
580 153–158 (2001).
- 581 **Reports modelling results that suggest that D–O variability is due to AMOC changes, and introduces the idea of**
582 **the AMOC flickering between three states.**
- 583 39. Menviel, L., Timmermann, A., Friedrich, T. & England, M. Hindcasting the continuum of Dansgaard-Oeschger variability:
584 Mechanisms, patterns and timing. *Clim. Past* **10**, 63–77 (2014).
- 585 40. Lynch-Stieglitz, J. The Atlantic Meridional Overturning Circulation and Abrupt Climate Change. *Annu. Rev. Mar. Sci.* **9**,
586 83–104 (2017).
- 587 41. Hoff, U., Rasmussen, T., Stein, R., Ezat, M. & Fahl, K. Sea ice and millennial-scale climate variability in the Nordic Seas
588 90 kyr to present. *Nat. Commun.* **7**, 12247 (2016).
- 589 42. Sadatzki, H. *et al.* Sea ice variability in the southern Norwegian Sea during glacial Dansgaard-Oeschger climate cycles.
590 *Sci. Adv.* **5**, eaau6174 (2019).
- 591 43. Wang, Y. *et al.* A high-resolution absolute-dated Late Pleistocene monsoon record from Hulu Cave, China. *Science* **294**,
592 2345–2348 (2001).
- 593 44. EPICA community members. One-to-one coupling of glacial climate variability in Greenland and Antarctica. *Nature* **444**,
594 195–198 (2006).
- 595 45. Deplazes, G. *et al.* Links between tropical rainfall and North Atlantic climate during the last glacial period. *Nat. Geosci.*
596 **6**, 213–217 (2013).
- 597 46. Ahn, J. & Brook, E. Siple Dome ice reveals two modes of millennial CO₂ change during the last ice age. *Nat. Commun.*
598 **5**, 3723 (2014).
- 599 47. Bond, G. & Lotti, R. Iceberg discharges into the North Atlantic on millennial time scales during the Last Glaciation.
600 *Science* **267**, 1005–1010 (1995).
- 601 48. Dokken, T. & Jansen, E. Rapid changes in the mechanism of ocean convection during the last glacial period. *Nature* **401**,
602 458–461 (1999).
- 603 49. van Kreveland, S. *et al.* Potential links between surging ice sheets, circulation changes, and the Dansgaard-Oeschger cycles
604 in the Irminger Sea, 60–18kyr. *Paleoceanography* **15**, 425–442 (2000).
- 605 50. Dickson, A. J., Austin, W. E. N., Hall, I. R., Maslin, M. A. & Kucera, M. Centennial-scale evolution of Dansgaard-
606 Oeschger events in the northeast Atlantic Ocean between 39.5 and 56.5 ka B.P. *Paleoceanography* **23**, [10.1029/
2008PA001595](https://doi.org/10.1029/2008PA001595) (2008).
- 607
- 608 51. Hodell, D., Evans, H., Channell, J. & Curtis, J. Phase relationships of North Atlantic ice-rafted debris and surface-deep
609 climate proxies during the last glacial period. *Quat. Sci. rev.* **29**, 3875–3886 (2010).
- 610 52. Manabe, S. & Stouffer, R. Simulation of abrupt climate change induced by freshwater input to the North Atlantic Ocean.
611 *Nature* **378**, 165–167 (1995).

- 612 **53.** Stouffer, R. *et al.* Investigating the causes of the response of the thermohaline circulation to past and future climate
613 changes. *J. Clim.* **19**, 1365–1387 (2006).
- 614 **54.** Broecker, W. S., Bond, G., Klas, M., Bonani, G. & Wolffi, W. A salt oscillator in the glacial Atlantic? 1. The concept.
615 *Paleoceanography* **5**, 469–477 (1990).
- 616 **55.** Peltier, W. R. & Vettoretti, G. Dansgaard-Oeschger oscillations predicted in a comprehensive model of glacial climate: A
617 "kicked" salt oscillator in the Atlantic. *Geophys. Res. Lett.* **41**, 7306–7313 (2014).
- 618 **56.** Brown, N. & Galbraith, E. D. Hosed vs. unhosed: interruptions of the Atlantic Meridional Overturning Circulation in a
619 global coupled model, with and without freshwater forcing. *Clim. Past* **12**, 1663–1679 (2016).
- 620 **57.** Vettoretti, G. & Peltier, W. R. Thermohaline instability and the formation of glacial North Atlantic super polynyas at the
621 onset of Dansgaard-Oeschger warming events. *Geophys. Res. Lett.* **43**, 5336–5344 (2016).
- 622 **58.** Klockmann, M., Mikolajewicz, U. & Marotzke, J. Two AMOC States in Response to Decreasing Greenhouse Gas
623 Concentrations in the Coupled Climate Model MPI-ESM. *J. Clim.* **31**, 7969–7984 (2018).
- 624 **59.** Zhang, X., Lohmann, G., Knorr, G. & Purcell, C. Abrupt glacial climate shifts controlled by ice sheet changes. *Nature*
625 **512**, 290–294 (2014).
- 626 **Shows that slow and moderate changes in LIS height or CO₂ concentration can trigger abrupt AMOC changes**
627 **in a fully coupled climate model.**
- 628 **60.** Zhang, X., Knorr, G., Lohmann, G. & Barker, S. Abrupt North Atlantic circulation changes in response to gradual CO₂
629 forcing in a glacial climate state. *Nat. Geosci.* **10**, 518–523 (2017).
- 630 **61.** Wolff, E., Chappellaz, J., Blunier, T., Rasmussen, S. & Svensson, A. Millennial-scale variability during the last glacial:
631 The ice core record. *Quat. Sci. Rev.* **29**, 2828 – 2838 (2010).
- 632 **62.** Allen, J. R. M. *et al.* Rapid environmental changes in southern Europe during the last glacial period. *Nature* **400**, 740–743
633 (1999).
- 634 **63.** Genty, D. *et al.* Precise dating of Dansgaard-Oeschger climate oscillations in western Europe from stalagmite data.
635 *Nature* **421**, 833–837 (2003).
- 636 **64.** Margari, V., Gibbard, P., Bryant, C. & Tzedakis, P. Character of vegetational and environmental changes in southern
637 Europe during the last glacial period; evidence from Lesvos Island, Greece. *Quat. Sci. Rev.* **28**, 1317 – 1339 (2009).
- 638 **65.** Cacho, I. *et al.* Dansgaard-Oeschger and Heinrich event imprints in Alboran Sea paleotemperatures. *Paleoceanography*
639 **14**, 698–705 (1999).
- 640 **66.** Martrat, B. *et al.* Abrupt temperature changes in the Western Mediterranean over the past 250,000 years. *Science* **306**,
641 1762–1765 (2004).
- 642 **67.** Rasmussen, T. L. & Thomsen, E. The role of the North Atlantic Drift in the millennial timescale glacial climate
643 fluctuations. *Palaeogeogr. Palaeoclimatol. Palaeoecol.* **210**, 101 – 116 (2004).
- 644 **68.** Böhm, E. *et al.* Strong and deep Atlantic meridional overturning circulation during the last glacial cycle. *Nature* **517**,
645 73–76 (2015).
- 646 **69.** Burckel, P. *et al.* Atlantic Ocean circulation changes preceded millennial tropical South America rainfall events during
647 the last glacial. *Geophys. Res. Lett.* **42**, 411–418 (2015).
- 648 **70.** Keigwin, L. D. & Boyle, E. A. Surface and deep ocean variability in the northern Sargasso Sea during marine isotope
649 stage 3. *Paleoceanography* **14**, 164–170 (1999).
- 650 **71.** Shackleton, N., Hall, M. & Vincent, E. Phase relationships between millennial-scale events 64,000-24,000 years ago.
651 *Paleoceanography* **15**, 565–569 (2000).

- 652 72. Skinner, L. C. & Elderfield, H. Rapid fluctuations in the deep North Atlantic heat budget during the last glacial period.
653 *Paleoceanography* **22**, [10.1029/2006PA001338](https://doi.org/10.1029/2006PA001338) (2007).
- 654 73. Lynch-Stieglitz, J. *et al.* Muted change in Atlantic overturning circulation over some glacial-aged Heinrich events. *Nat.*
655 *Geosci.* **7**, 144–150 (2014).
- 656 74. Piotrowski, A., Goldstein, S., S.R.Hemming & Fairbanks, R. Temporal relationships of carbon cycling and ocean
657 circulation glacial boundaries. *Science* **307**, 1933–1938 (2005).
- 658 75. Piotrowski, A., Goldstein, S., S.R.Hemming, Fairbanks, R. & Zylberberg, D. Oscillating glacial northern and southern
659 deep water formation from combined neodymium and carbon isotopes. *Earth Planet. Sci. Lett.* **272**, 394–405 (2008).
- 660 76. Gottschalk, J. *et al.* Abrupt changes in the southern extent of North Atlantic DeepWater during Dansgaard-Oeschger
661 events. *Nat. Geosci.* **8**, 950–954 (2015).
- 662 77. Trenberth, K. & Caron, J. Estimates of meridional atmosphere and ocean heat transports. *J. Clim.* **14**, 3433–3443 (2001).
- 663 78. Johns, W. E. *et al.* Continuous, array-based estimates of atlantic ocean heat transport at 26.5°N. *J. Clim.* **24**, 2429–2449
664 (2011).
- 665 79. Kageyama, M. *et al.* Climatic impacts of fresh water hosing under Last Glacial Maximum conditions: a multi-model
666 study. *Clim. Past* **9**, 935–953 (2013).
- 667 80. Li, C., Battisti, D., Schrag, D. & Tziperman, E. Abrupt climate shifts in Greenland due to displacements of the sea ice
668 edge. *Geophys. Res. Lett.* **32**, L19702 (2005).
- 669 81. Dokken, T., Nisancioglu, K., Li, C., Battisti, D. & Kissel, C. Dansgaard-Oeschger cycles: Interactions between ocean and
670 sea ice intrinsic to the Nordic seas. *Paleoceanography* **28**, 491–502 (2013).
- 671 **Presents observational evidence for the expression of D–O variability in the Nordic Sea, highlighting the possibil-**
672 **ity of the occurrence of convective overturning events.**
- 673 82. Ezat, M. M., Rasmussen, T. L. & Groeneveld, J. Persistent intermediate water warming during cold stadials in the
674 southeastern Nordic seas during the past 65 k.y. *Geology* **42**, 663–666 (2014).
- 675 83. Müller, J. & Stein, R. High-resolution record of late glacial and deglacial sea ice changes in Fram Strait corroborates
676 ice-ocean interactions during abrupt climate shifts. *Earth Planet. Sci. Lett.* **403**, 446–455 (2014).
- 677 84. He, C. *et al.* North Atlantic subsurface temperature response controlled by effective freshwater input in "Heinrich" events.
678 *Earth Planet. Sci. Lett.* **539**, 116247 (2020).
- 679 85. Trenberth, K. E. & Fasullo, J. T. Atlantic meridional heat transports computed from balancing Earth's energy locally.
680 *Geophys. Res. Lett.* **44**, 1919–1927 (2017).
- 681 86. Berger, W. & Wefer, G. *The South Atlantic* (Springer, Berlin, 1996).
- 682 87. Schmittner, A., Saenko, O. & Weaver, A. Coupling of the hemispheres in observations and simulations of glacial climate
683 change. *Quat. Sci. Rev.* **22**, 659–671 (2003).
- 684 88. Stocker, T. & Johnsen, S. A minimum thermodynamic model for the bipolar seesaw. *Paleoceanography* **18**, 1087,
685 [doi:10.1029/2003PA000920](https://doi.org/10.1029/2003PA000920) (2003).
- 686 89. Barker, S. & Diz, P. Timing of the descent into the last Ice Age determined by the bipolar seesaw. *Paleoceanography* **29**,
687 489–507 (2014).
- 688 90. Gottschalk, J., Skinner, L. C. & Waelbroeck, C. Contribution of seasonal sub-Antarctic surface water variability to
689 millennial-scale changes in atmospheric CO₂ over the last deglaciation and Marine Isotope Stage 3. *Earth Planet. Sci.*
690 *Lett.* **411**, 87 – 99 (2015).

- 691 **91.** Gottschalk, J. *et al.* Southern Ocean link between changes in atmospheric CO₂ levels and northern-hemisphere climate
692 anomalies during the last two glacial periods. *Quat. Sci. Rev.* **230**, 106067 (2020).
- 693 **92.** Kaiser, J., Lamy, F. & Hebbeln, D. A 70-kyr sea surface temperature record off Southern Chile. *Paleoceanography* **20**,
694 [10.1029/2004PA001146](https://doi.org/10.1029/2004PA001146) (2005).
- 695 **93.** Pahnke, K., Zahn, R., Elderfield, H. & Schulz, M. 340,000-year centennial-scale marine record of Southern Hemisphere
696 climatic oscillation. *Science* **301**, 948–952 (2003).
- 697 **94.** Caniupán, M. *et al.* Millennial-scale sea surface temperature and Patagonian Ice Sheet changes off southernmost Chile
698 (53°S) over the past 60 kyr. *Paleoceanography* **26**, [10.1029/2010PA002049](https://doi.org/10.1029/2010PA002049) (2011).
- 699 **95.** Blunier, T. & Brook, E. Timing of millennial-scale climate change in Antarctica and Greenland during the last glacial
700 period. *Science* **291**, 109–112 (2001).
- 701 **96.** Parrenin, F. *et al.* Synchronous change of atmospheric CO₂ and Antarctic temperature during the last deglacial warming.
702 *Science* **339**, 1060–1063 (2013).
- 703 **97.** Buizert, C. & Members, W. D. P. Precise inter-polar phasing of abrupt climate change during the last ice age. *Nature* **520**,
704 661–665 (2015).
- 705 **Shows that Greenland temperature changes lead Antarctic temperature changes by ~200 years, suggesting North**
706 **Atlantic control of D–O variability and an oceanic teleconnection to high southern latitudes.**
- 707 **98.** Broecker, W. Paleocirculation during the last deglaciation: A bipolar seesaw? *Paleoceanography* **13**, 119–121
708 (1998).
- 709 **99.** Sánchez-Goñi, M., Turon, J.-L., Eynaud, F. & Gendreau, S. European Climatic Response to Millennial-Scale Changes in
710 the Atmosphere–Ocean System during the Last Glacial Period. *Quat. Res.* **54**, 394–403 (2000).
- 711 **100.** Sánchez-Goñi, M. *et al.* Synchronicity between marine and terrestrial responses to millennial scale climatic variability
712 during the last glacial period in the Mediterranean region. *Clim. Dyn.* **19**, 95–105 (2002).
- 713 **101.** Tzedakis, P. *et al.* Ecological thresholds and patterns of millennial-scale climate variability: The response of vegetation in
714 Greece during the last glacial period. *Geology* **32**, 109–112 (2004).
- 715 **102.** Stockhecke, M. *et al.* Millennial to orbital-scale variations of drought intensity in the Eastern Mediterranean. *Quat. Sci.*
716 *Rev.* **133**, 77 – 95 (2016).
- 717 **103.** Wang, X. *et al.* Millennial-scale precipitation changes in southern Brazil over the past 90,000 years. *Geophys. Res. Lett.*
718 **34**, L23701 (2007).
- 719 **104.** Kanner, L., Burns, S., Cheng, H. & Edwards, R. L. High-Latitude Forcing of the South American Summer Monsoon
720 During the Last Glacial. *Science* **335**, 570–573 (2013).
- 721 **105.** Mosblech, N. *et al.* North Atlantic forcing of Amazonian precipitation during the last ice age. *Nat. Geosci.* **5**, 817–820
722 (2012).
- 723 **106.** Ivanochko, T. *et al.* Variations in tropical convection as an amplifier of global climate change at the millennial scale.
724 *Earth Planet. Sci. Lett.* **235**, 302–314 (2005).
- 725 **107.** Pausata, F., Battisti, D., Nisancioglu, K. & Bitz, C. Chinese stalagmite $\delta^{18}\text{O}$ controlled by changes in the Indian monsoon
726 during a simulated Heinrich event. *Nat. Geosci.* **4**, 474–480 (2011).
- 727 **108.** Marzin, C., Kallel, N., Kageyama, M., Duplessy, J.-C. & Braconnot, P. Glacial fluctuations of the Indian monsoon and
728 their relationship with North Atlantic climate: new data and modelling experiments. *Clim. Past* **9**, 2135–2151 (2013).
- 729 **109.** Lauterbach, S. *et al.* A ~130 kyr record of surface water temperature and $\delta^{18}\text{O}$ from the northern Bay of Bengal -
730 investigating the linkage between Heinrich events and Weak Monsoon Intervals in Asia. *Paleoceanogr. Paleoclimatology*
731 **35**, e2019PA003646 (2020).

- 732 **110.** Wang, Y. *et al.* Millennial- and orbital-scale changes in the East Asian monsoon over the past 224,000 years. *Nature* **451**,
733 1090–1093 (2008).
- 734 **111.** Cheng, H. *et al.* Ice age terminations. *Science* **326**, 248–252 (2009).
- 735 **112.** Schneider, T., Bischoff, T. & Haug, G. Migrations and dynamics of the intertropical convergence zone. *Nature* **513**,
736 45–53 (2014).
- 737 **113.** Broecker, W., Peteet, D. & Rind, D. Does the ocean-atmosphere system have more than one stable mode of operation?
738 *Nature* **315**, 21–26 (1985).
739 **One of the first suggestions that the millennial-scale temperature changes observed in Greenland ice cores and**
740 **in Europe are due to changes in NADW formation and that there could be two quasi-stable modes in the climate**
741 **system.**
- 742 **114.** Menviel, L., Timmermann, A., Mouchet, A. & Timm, O. Climate and marine carbon cycle response to changes in the
743 strength of the southern hemispheric westerlies. *Paleoceanography* **23**, [10.1029/2007PA001604](https://doi.org/10.1029/2007PA001604) (2008).
- 744 **115.** Marcott, S. *et al.* Ice-shelf collapse from subsurface warming as trigger for Heinrich events. *Proc. Natl. Acad. Sci. USA*
745 **108**, 13415–13419 (2011).
746 **Provides evidence for sub-surface warming in the North Atlantic during stadials and suggests that this warming**
747 **led to a destabilization of the LIS.**
- 748 **116.** Rainsley, E. *et al.* Greenland ice mass loss during the Younger Dryas driven by Atlantic Meridional Overturning
749 Circulation feedbacks. *Sci. Reports* **8**, 11307 (2018).
- 750 **117.** McManus, J. F., Francois, R., Gherardi, J. M., Keigwin, L. D. & Brown-Leger, S. Collapse and rapid resumption of
751 Atlantic meridional circulation linked to deglacial climate changes. *Nature* **428**, 834–837 (2004).
- 752 **118.** Curry, W. B. & Oppo, D. W. Synchronous, high-frequency oscillations in tropical sea surface temperatures and North
753 Atlantic Deep Water production during the Last Glacial Cycle. *Paleoceanography* **12**, 1–14 (1997).
- 754 **119.** Vidal, L. *et al.* Evidence for changes in the North Atlantic Deep Water linked to meltwater surges during the Heinrich
755 events. *Earth Planet. Sci. Lett.* **146**, 13–27 (1997).
- 756 **120.** Zahn, R. *et al.* Thermohaline instability in the North Atlantic during meltwater events: Stable isotope and ice-rafted
757 detritus records from core SO75-26KL, Portuguese margin. *Paleoceanography* **12**, 696–710 (1997).
- 758 **121.** Weldeab, S., Lea, D., Schneider, R. & Andersen, N. 155,000 years of West African Monsoon and ocean thermal evolution.
759 *Science* **316**, 1303–1307 (2007).
- 760 **122.** Hodell, D. *et al.* An 85-ka record of climate change in lowland Central America. *Quat. Sci. rev.* **27**, 1152–1165 (2008).
- 761 **123.** Cai, Y. *et al.* Variability of stalagmite-inferred Indian monsoon precipitation over the past 252,000 y. *Proc. Natl. Acad.*
762 *Sci.* **112**, 2954–2959 (2015).
- 763 **124.** Wang, X. *et al.* Wet periods in northeastern Brazil over the past 210 kyr linked to distant climate anomalies. *Nature* **432**,
764 740–743 (2004).
- 765 **125.** Leduc, G. *et al.* Moisture transport across Central America as a positive feedback on abrupt climatic changes. *Nature*
766 **445**, 908–911 (2007).
- 767 **126.** Carolin, S. A. *et al.* Varied Response of Western Pacific Hydrology to Climate Forcings over the Last Glacial Period.
768 *Science* **340**, 1564–1566 (2013).
- 769 **127.** Timmermann, A. *et al.* Towards a quantitative understanding of millennial-scale Antarctic warming events. *Quat. Sci.*
770 *Rev.* **29**, 74–85 (2010).

- 771 **128.** Buiron, D. *et al.* Regional imprints of millennial variability during the MIS 3 period around Antarctica. *Quat. Sci. Rev.*
772 **48**, 99–112 (2012).
- 773 **129.** Skinner, L., Waelbroeck, C., Scrivner, A. & Fallon, S. Radiocarbon evidence for alternating northern and southern sources
774 of ventilation of the deep Atlantic carbon pool during the last deglaciation. *Proc. Natl. Acad. Sci. USA* **111**, 5480–5484
775 (2014).
- 776 **130.** Gottschalk, J. *et al.* Biological and physical controls in the Southern Ocean on past millennial-scale atmospheric CO₂
777 changes. *Nat. Commun.* **7**, 11539 (2016).
- 778 **131.** Jaccard, S., Galbraith, E., Martinez-Garcia, A. & Anderson, R. Covariation of deep Southern Ocean oxygenation and
779 atmospheric CO₂ through the last ice age. *Nature* **530**, 207–210 (2016).
- 780 **132.** Menviel, L., Spence, P. & England, M. Contribution of enhanced Antarctic Bottom Water formation to Antarctic warm
781 events and millennial-scale atmospheric CO₂ increase. *Earth Planet. Sci. Lett.* **413**, 37–50 (2015).
- 782 **133.** Pedro, J. B. *et al.* Southern Ocean deep convection as a driver of Antarctic warming events. *Geophys. Res. Lett.* **43**,
783 2192–2199 (2016).
- 784 **134.** Menviel, L. *et al.* Southern Hemisphere westerlies as a driver of the early deglacial atmospheric CO₂ rise. *Nat. Commun.*
785 **9**, 2503 (2018).
- 786 **135.** Pedro, J. B. *et al.* Beyond the bipolar seesaw: Toward a process understanding of interhemispheric coupling. *Quat. Sci.*
787 *Rev.* **192**, 27 – 46 (2018).
- 788 **136.** Hwang, Y.-T., Frierson, D. M. W. & Kang, S. M. Anthropogenic sulfate aerosol and the southward shift of tropical
789 precipitation in the late 20th century. *Geophys. Res. Lett.* **40**, 2845–2850 (2013).
- 790 **137.** Ceppi, P., Hwang, Y.-T., Liu, X., Frierson, D. & Hartmann, D. The relationship between the ITCZ and the Southern
791 Hemispheric eddy-driven jet. *J. Geophys. Res. Atmospheres* **118**, 5136–5146 (2013).
- 792 **138.** Lee, S.-Y., Chiang, J. C. H., Matsumoto, K. & Tokos, K. S. Southern Ocean wind response to North Atlantic cooling and
793 the rise in atmospheric CO₂: modeling perspective and paleoceanographic implications. *Paleoceanography* **26**, PA1214,
794 [10.1029/2010PA002004](https://doi.org/10.1029/2010PA002004) (2011).
- 795 **139.** Buizert, C. *et al.* Abrupt ice-age shifts in southern westerly winds and Antarctic climate forced from the north. *Nature*
796 **563**, 681–685 (2018).
- 797 **140.** Toggweiler, J., Russell, J. & Carson, S. Midlatitude westerlies, atmospheric CO₂, and climate change during ice ages.
798 *Paleoceanography* **21**, PA2005, [10.1029/2005PA001154](https://doi.org/10.1029/2005PA001154) (2006).
- 799 **141.** Ahn, J. & Brook, E. Atmospheric CO₂ and climate on Millennial Time Scales During the Last Glacial Period. *Science*
800 **322**, 83–85 (2008).
- 801 **142.** Stein, K., Timmermann, A., Kwon, E. Y. & Friedrich, T. Timing and magnitude of Southern Ocean sea ice/carbon cycle
802 feedbacks. *Proc. Natl. Acad. Sci. USA* **117**, 4498–4504 (2020).
- 803 **143.** Okazaki, Y. *et al.* Deep water formation in the North Pacific during the Last Glacial termination. *Science* **329**, 200–204
804 (2010).
- 805 **144.** Max, L. *et al.* Pulses of enhanced north pacific intermediate water ventilation from the okhotsk sea and bering sea during
806 the last deglaciation. *Clim. Past* **10**, 591–605 (2014).
- 807 **145.** Zheng, X. *et al.* Deepwater circulation variation in the South China Sea since the Last Glacial Maximum. *Geophys. Res.*
808 *Lett.* **43**, 8590–8599 (2016).
- 809 **146.** Saenko, O., Schmittner, A. & Weaver, A. The Atlantic-Pacific seesaw. *J. Clim.* **17**, 2033–2038 (2004).

- 810 **147.** Chikamoto, M. *et al.* Variability in North Pacific intermediate and deep water ventilation during Heinrich events in two
811 coupled climate models. *Deep. Sea Res. II* **61-64**, 114–126 (2012).
- 812 **148.** Gong, X. *et al.* Enhanced North Pacific deep-ocean stratification by stronger intermediate water formation during Heinrich
813 Stadial 1. *Nat Commun* **10**, 656 (2019).
- 814 **149.** Menviel, L., England, M., Meissner, K., Mouchet, A. & Yu, J. Atlantic-Pacific seesaw and its role in outgassing CO₂
815 during Heinrich events. *Paleoceanography* **29**, 58–70 (2014).
- 816 **150.** Rasmussen, T., Thomsen, E., Labeyrie, L. & van Weering, T. Circulation changes in the Faeroe-Shetland Channel
817 correlating with cold events during the last glacial period (58 -10 ka). *Geology* **24**, 937–940 (1996).
- 818 **151.** Kissel, C., Laj, C., Piotrowski, A., Goldstein, S. & Hemming, S. Millennial-scale propagation of Atlantic deep waters to
819 the glacial Southern Ocean. *Paleoceanography* **23**, PA2102, doi:10.1029/2008PA001624 (2008).
- 820 **152.** Fleitmann, D. *et al.* Timing and climatic impact of Greenland interstadials recorded in stalagmites from northern Turkey.
821 *Geophys. Res. Lett.* **36**, L19707, 10.1029/2009GL040050 (2009).
- 822 **153.** Fletcher, W. *et al.* Millennial-scale variability during the last glacial in vegetation records from Europe. *Quat. Sci. Rev.*
823 **29**, 2839 – 2864 (2010).
- 824 **154.** Müller, U. *et al.* The role of climate in the spread of modern humans into Europe. *Quat. Sci. Rev.* **30**, 273 – 279 (2011).
- 825 **155.** Brook, E. J., Harder, S., Severinghaus, J., Steig, E. & Sucher, C. On the origin and timing of rapid changes in atmospheric
826 methane during the last glacial period. *Glob. Biogeochem. Cycles* **14**, 559–572 (2000).
- 827 **156.** Chappellaz, J. *et al.* Synchronous changes in atmospheric CH₄ and Greenland climate between 40 and 8 kyr BP. *Nature*
828 **366**, 443–445 (1993).
- 829 **157.** Brook, E. J., Sowers, T. & Orchardo, J. Rapid Variations in Atmospheric Methane Concentrations During the Past 110,000
830 Years. *Science* **273**, 1087–1091 (1996).
- 831 **158.** Bergamaschi, P. *et al.* Satellite cartography of atmospheric methane from SCIAMACHY on board ENVISAT: 2.
832 Evaluation based on inverse model simulations. *J. Geophys. Res. Atmospheres* **112**, 10.1029/2006JD007268 (2007).
- 833 **159.** Rhodes, R. *et al.* Enhanced tropical methane production in response to iceberg discharge in the North Atlantic. *Science*
834 **348**, 1016–1019 (2015).
- 835 **160.** Tzedakis, P., Pälike, H., Roucoux, K. & de Abreu, L. Atmospheric methane, southern European vegetation and low-mid
836 latitude links on orbital and millennial timescales. *Earth Planet. Sci. Lett.* **277**, 307 – 317 (2009).
- 837 **161.** Timmermann, A., Schulz, M., Gildor, H. & Tziperman, E. Coherent resonant millennial-scale climate oscillations
838 triggered by massive meltwater pulses. *J. Clim.* **16**, 2569–2585 (2003).
- 839 **162.** Alley, R. B., Anandakrishnan, S. & Jung, P. Stochastic resonance in the North Atlantic. *Paleoceanography* **16**, 190–198
840 (2001).
- 841 **163.** Ganopolski, A. & Rahmstorf, S. Abrupt Glacial Climate Changes due to Stochastic Resonance. *Phys. Rev. Lett.* **88**,
842 038501 (2002).
- 843 **164.** Krebs, U. & Timmermann, A. Tropical air-sea interactions accelerate the recovery of the Atlantic Meridional Overturning
844 Circulation after a major shutdown. *J. Clim.* **20**, 4940–4956 (2007).
- 845 **165.** Richter, I. & Xie, S.-P. Moisture transport from the Atlantic to the Pacific basin and its response to North Atlantic cooling
846 and global warming. *Clim. Dyn.* **35**, 551–566 (2010).
- 847 **166.** Friedrich, T. *et al.* The mechanism behind internally generated centennial-to-millennial scale climate variability in an
848 earth system model of intermediate complexity. *Geosci. Model. Dev.* **3**, 377–389 (2010).

- 849 **167.** Drijfhout, S., Gleeson, E., Dijkstra, H. A. & Livina, V. Spontaneous abrupt climate change due to an atmospheric
850 blocking–sea-ice–ocean feedback in an unforced climate model simulation. *Proc. Natl. Acad. Sci. USA* **110**, 19713–19718
851 (2013).
- 852 **168.** Kleppin, H., Jochum, M., Otto-Bliesner, B., Shields, C. A. & Yeager, S. Stochastic Atmospheric Forcing as a Cause of
853 Greenland Climate Transitions. *J. Clim.* **28**, 7741–7763 (2015).
- 854 **169.** Singh, H. A., Battisti, D. S. & Bitz, C. M. A Heuristic Model of Dansgaard-Oeschger Cycles. Part I: Description, Results,
855 and Sensitivity Studies. *J. Clim.* **27**, 4337–4358 (2014).
- 856 **170.** Petersen, S., Schrag, D. & Clark, P. A new mechanism for Dansgaard-Oeschger cycles. *Paleoceanography* **28**, 1–7
857 (2013).
- 858 **171.** Boers, N., Ghil, M. & Rousseau, D.-D. Ocean circulation, ice shelf, and sea ice interactions explain Dansgaard-Oeschger
859 cycles. *Proc. Natl. Acad. Sci.* **115**, E11005–E11014 (2018).
- 860 **172.** Hulbe, C. L., MacAyeal, D. R., Denton, G. H., Kleman, J. & Lowell, T. V. Catastrophic ice shelf breakup as the source of
861 Heinrich event icebergs. *Paleoceanography* **19**, [10.1029/2003PA000890](https://doi.org/10.1029/2003PA000890) (2004).
- 862 **173.** Cofaigh, C. *et al.* The role of meltwater in high-latitude trough-mouth fan development: The Disko Trough-Mouth Fan,
863 West Greenland. *Mar. Geol.* **402**, 17 – 32 (2018).
- 864 **174.** Jennings, A. E. *et al.* Baffin Bay paleoenvironments in the LGM and HS1: Resolving the ice-shelf question. *Mar. Geol.*
865 **402**, 5 – 16 (2018).
- 866 **175.** Obase, T. & Abe-Ouchi, A. Abrupt Bolling-Allerod Warming Simulated under Gradual Forcing of the Last Deglaciation.
867 *Geophys. Res. Lett.* **46**, 11397–11405 (2019).
- 868 **176.** Guo, C., Nisancioglu, K. H., Bentsen, M., Bethke, I. & Zhang, Z. Equilibrium simulations of Marine Isotope Stage 3
869 climate. *Clim. Past* **15**, 1133–1151 (2019).
- 870 **177.** Marshall, S. & Koutnik, M. Ice sheet action versus reaction: distinguishing between Heinrich events and Dansgaard-
871 Oeschger cycles in the North Atlantic. *Paleoceanography* **21**, PA2021 (2006).
- 872 **178.** Alvarez-Solas, J., Banderas, R., Robinson, A. & Montoya, M. Ocean-driven millennial-scale variability of the Eurasian
873 ice sheet during the last glacial period simulated with a hybrid ice-sheet–shelf model. *Clim. Past* **15**, 957–979 (2019).
- 874 **179.** Zhang, X., Prange, M., Merkel, U. & Schulz, M. Instability of the Atlantic overturning circulation during Marine Isotope
875 Stage 3. *Geophys. Res. Lett.* **41**, 4285–4293 (2014).
- 876 **180.** Yokoyama, Y., Esat, T. & Lambeck, K. Coupled climate and sea-level changes deduced from Huon Peninsula coral
877 terraces of the last ice age. *Earth Planet. Sci. Lett.* **193**, 579–587 (2001).
- 878 **181.** Chappell, J. Sea level changes forced ice breakouts in the last glacial cycle: New results from coral terraces. *Quat. Sci.*
879 *Rev.* **21**, 1229–1240 (2002).
- 880 **182.** Rohling, E., Marsh, R., Wells, N., Siddall, M. & Edwards, N. Similar meltwater contributions to glacial sea level changes
881 from Antarctic and northern ice sheets. *Nature* **430**, 1016–1021 (2004).
- 882 **183.** Arz, H. W., Lamy, F., Ganopolski, A., Nowaczyk, N. & Pätzold, J. Dominant Northern Hemisphere climate control over
883 millennial-scale glacial sea-level variability. *Quat. Sci. Rev.* **26**, 312 – 321 (2007).
- 884 **184.** MacAyeal, D. Binge/purge oscillations of the Laurentide ice sheet as a cause of the North Atlantic’s Heinrich events.
885 *Paleoceanography* **8**, 775–784 (1993).
- 886 **Suggests that Heinrich events are due to growth–purge oscillations of the LIS.**
- 887 **185.** Calov, R., Ganopolski, A., Petoukhov, V., Claussen, M. & Greve, R. Large-scale instabilities of the Laurentide ice sheet
888 simulated in a fully coupled climate-system model. *Geophys. Res. Lett.* **29**, 69–1–69–4 (2002).

- 889 **186.** Calov, R. *et al.* Results from the Ice-Sheet Model Intercomparison Project-Heinrich Event INtercOmparison (ISMIP
890 HEINO). *J. Glaciol.* **56**, 371–383 (2010).
- 891 **187.** Shaffer, G., Olsen, S. & Bjerrum, C. Ocean subsurface warming as a mechanism for coupling Dansgaard-Oeschger
892 climate cycles and ice-rafting events. *Geophys. Res. Lett.* **31**, L24202 (2004).
- 893 **188.** Mignot, J., Ganopolski, A. & Levermann, A. Atlantic subsurface temperatures: Response to a shutdown of the overturning
894 circulation and consequences for its recovery. *J. Clim.* **20**, 4884–4898 (2007).
- 895 **189.** Massom, R. *et al.* Antarctic ice shelf disintegration triggered by sea ice loss and ocean swell. *Nature* **558**, 383–389
896 (2018).
- 897 **190.** Greene, C. A., Young, D. A., Gwyther, D. E., Galton-Fenzi, B. K. & Blankenship, D. D. Seasonal dynamics of totten ice
898 shelf controlled by sea ice buttressing. *The Cryosphere* **12**, 2869–2882 (2018).
- 899 **191.** Alvarez-Solas, J. *et al.* Links between ocean temperature and iceberg discharge during Heinrich events. *Nat. Geosci.* **3**,
900 122–126 (2010).
- 901 **192.** Alvarez-Solas, J., Robinson, A., Montoya, M. & Ritz, C. Iceberg discharges of the last glacial period driven by oceanic
902 circulation changes. *Proc. Natl. Acad. Sci. USA* **110**, 16350–16354 (2013).
- 903 **193.** Tabone, I., Robinson, A., Alvarez-Solas, J. & Montoya, M. Impact of millennial-scale oceanic variability on the Greenland
904 ice-sheet evolution throughout the last glacial period. *Clim. Past* **15**, 593–609 (2019).
- 905 **194.** Bassis, J., Petersen, S. & Cathles, L. M. Heinrich events triggered by ocean forcing and modulated by isostatic adjustment.
906 *Nature* **542**, 332–334 (2017).
- 907 **195.** Roberts, W. H. G., Valdes, P. J. & Payne, A. J. Topography’s crucial role in Heinrich Events. *Proc. Natl. Acad. Sci. USA*
908 **111**, 16688–16693 (2014).
- 909 **196.** Andres, H. J. & Tarasov, L. Towards understanding potential atmospheric contributions to abrupt climate changes:
910 characterizing changes to the North Atlantic eddy-driven jet over the last deglaciation. *Clim. Past* **15**, 1621–1646 (2019).
- 911 **197.** Zieme, F. A., Kapsch, M.-L., Klockmann, M. & Mikolajewicz, U. Heinrich events show two-stage climate response in
912 transient glacial simulations. *Clim. Past* **15**, 153–168 (2019).
- 913 **198.** Carlson, A. E., Tarasov, L. & Pico, T. Rapid Laurentide ice-sheet advance towards southern last glacial maximum limit
914 during marine isotope stage 3. *Quat. Sci. Rev.* **196**, 118 – 123 (2018).
- 915 **199.** Clark, P. U. *et al.* Freshwater Forcing of Abrupt Climate Change During the Last Glaciation. *Science* **293**, 283–287
916 (2001).
- 917 **200.** Galaasen, E. V. *et al.* Rapid reductions in north atlantic deep water during the peak of the last interglacial period. *Science*
918 **343**, 1129–1132 (2014).
- 919 **201.** Tzedakis, P. *et al.* Enhanced climate instability in the North Atlantic and southern Europe during the Last Interglacial.
920 *Nat. Commun.* **9**, 4235 (2018).
- 921 **202.** Galaasen, E. V. *et al.* Interglacial instability of north atlantic deep water ventilation. *science* **367**, 1485–1489 (2020).
- 922 **203.** Irvali, N. *et al.* Evidence for regional cooling, frontal advances, and East Greenland Ice Sheet changes during the demise
923 of the last interglacial. *Quat. Sci. Rev.* **150**, 184–199 (2016).
- 924 **204.** Oka, A., Hasumi, H. & Abe-Ouchi, A. The thermal threshold of the atlantic meridional overturning circulation and its
925 control by wind stress forcing during glacial climate. *Geophys. Res. Lett.* **39**, [10.1029/2012GL051421](https://doi.org/10.1029/2012GL051421) (2012).
- 926 **205.** Hu, A. *et al.* Role of the Bering Strait on the hysteresis of the ocean conveyor belt circulation and glacial climate stability.
927 *Proc. Natl. Acad. Sci. USA* **107**, 6417–6422 (2012).

- 928 **206.** Hu, A. *et al.* Effects of the Bering Strait closure on AMOC and global climate under different background climates. *Prog.*
929 *Oceanogr.* **132**, 174 – 196 (2015).
- 930 **207.** de Boer, A. M. & Nof, D. The Exhaust Valve of the North Atlantic. *J. Clim.* **17**, 417–422 (2004).
- 931 **208.** Menviel, L. *et al.* Removing the North Pacific halocline: effects on global climate, ocean circulation and the carbon cycle.
932 *Deep. Sea Res. Part II* **61-64**, 106–113 (2012).
- 933 **209.** Curry, W. & Oppo, D. Glacial water mass geometry and the distribution of $\delta^{13}\text{C}$ of ΣCO_2 in the western Atlantic Ocean.
934 *Paleoceanography* **20**, [10.1029/2004PA001021](https://doi.org/10.1029/2004PA001021) (2005).
- 935 **210.** Marchitto, T. & Broecker, W. Deep water mass geometry in the glacial Atlantic Ocean: A review of constraints from the
936 paleonutrient proxy Cd/Ca. *Geochem. Geophys. Geosystems* **7**, [10.1029/2006GC001323](https://doi.org/10.1029/2006GC001323) (2006).
- 937 **211.** Lynch-Stieglitz, J. *et al.* Meridional overturning circulation in the South Atlantic at the last glacial maximum. *Geochem.*
938 *Geophys. Geosystems* **7**, [10.1029/2005GC001226](https://doi.org/10.1029/2005GC001226) (2006).
- 939 **212.** Menviel, L. *et al.* Poorly ventilated deep ocean at the Last Glacial Maximum inferred from carbon isotopes: a data-model
940 comparison study. *Paleoceanography* **32**, 2–17 (2017).
- 941 **213.** Skinner, L. *et al.* Radiocarbon constraints on the glacial ocean circulation and its impact on atmospheric CO_2 . *Nat.*
942 *Commun.* **8**, 16010 (2017).
- 943 **214.** Muglia, J. & Schmittner, A. Glacial Atlantic overturning increased by wind stress in climate models. *Geophys. Res. Lett.*
944 **42**, 9862–9868 (2015).
- 945 **215.** Kageyama, M. *et al.* The PMIP4-CMIP6 Last Glacial Maximum experiments: preliminary results and comparison with
946 the PMIP3-CMIP5 simulations. *Clim. Past Discuss.* **2020**, 1–37 (2020).
- 947 **216.** Sherriff-Tadano, S., Abe-Ouchi, A., Yoshimori, M., Oka, A. & Chan, W.-L. Influence of glacial ice sheets on the Atlantic
948 meridional overturning circulation through surface wind change. *Clim. Dyn.* **50**, 2881–2903 (2018).
- 949 **217.** Born, A. & Stocker, T. F. Two Stable Equilibria of the Atlantic Subpolar Gyre. *J. Phys. Oceanogr.* **44**, 246–264 (2014).
- 950 **218.** Li, C. & Born, A. Coupled atmosphere-ice-ocean dynamics in Dansgaard-Oeschger events. *Quat. Sci. Rev.* **203**, 1 – 20
951 (2019).
- 952 **219.** Heuzé, C. North atlantic deep water formation and amoc in cmip5 models. *Ocean. Sci.* **13**, 609–622 (2017).
- 953 **220.** Jensen, M. F., Nisancioglu, K. H. & Spall, M. A. Large Changes in Sea Ice Triggered by Small Changes in Atlantic Water
954 Temperature. *J. Clim.* **31**, 4847–4863 (2018).
- 955 **221.** Menviel, L. C. *et al.* Enhanced Mid-depth Southward Transport in the Northeast Atlantic at the Last Glacial Maximum
956 Despite a Weaker AMOC. *Paleoceanogr. Paleoclimatology* **35**, e2019PA003793 (2020).
- 957 **222.** Toggweiler, J. & Samuels, B. Effect of Drake passage on the global thermohaline circulation. *Deep. Sea Res. I* **42**,
958 477–500 (1995).
- 959 **223.** Delworth, T. L. & Zeng, F. Simulated impact of altered Southern Hemisphere winds on the Atlantic Meridional
960 Overturning Circulation. *Geophys. Res. Lett.* **35** (2008).
- 961 **224.** Gent, P. R. Effects of Southern Hemisphere Wind Changes on the Meridional Overturning Circulation in Ocean Models.
962 *Annu. Rev. Mar. Sci.* **8**, 79–94 (2016). PMID: 26163010.
- 963 **225.** Swingedouw, D., Fichefet, T., Goosse, H. & Loutre, M.-F. Impact of transient freshwater releases in the Southern Ocean
964 on the AMOC and climate. *Clim. Dyn.* **33**, 365–381 (2009).
- 965 **226.** Martin, T., Park, W. & Latif, M. Multi-centennial variability controlled by Southern Ocean convection in the Kiel Climate
966 Model. *Clim. Dyn.* **40**, 2005–2022 (2013).

- 967 **227.** Bond, G. *et al.* A Pervasive Millennial-Scale Cycle in North Atlantic Holocene and Glacial Climates. *Science* **278**,
968 1257–1266 (1997).
- 969 **228.** Schulz, M., Paul, A. & Timmermann, A. Relaxation oscillators in concert: A framework for climate change at millennial
970 timescales during the late Pleistocene. *Geophys. Res. Lett.* **29**, 46–1–46–4 (2002).
- 971 **229.** Svensson, A. *et al.* A 60,000 year Greenland stratigraphic ice core chronology. *Clim. Past* **4**, 47–57 (2008).
- 972 **230.** Bereiter, B. *et al.* Mode of change of millennial CO₂ variability during the last glacial cycle associated with a bipolar
973 marine carbon seesaw. *Proc. Natl Acad. Sci. USA* **109**, 9755–9760 (2012).
- 974 **231.** Locarnini, R. *et al.* *World Ocean Atlas 2013*, vol. 1, 40 (NOAA Atlas NESDIS 73, 2013).
- 975 **232.** Bullister, J. L., Rhein, M. & Mauritzen, C. In Siedler, G., Griffies, S. M., Gould, J. & Church, J. A. (eds.) *Ocean Circulation*
976 *and Climate*, vol. 103 of *International Geophysics*, chap. 10, 227 – 253, [https://doi.org/10.1016/B978-0-12-391851-2.](https://doi.org/10.1016/B978-0-12-391851-2.00010-6)
977 [00010-6](https://doi.org/10.1016/B978-0-12-391851-2.00010-6) (Academic Press, 2013).
- 978 **233.** Cunningham, S. A. *et al.* Temporal Variability of the Atlantic Meridional Overturning Circulation at 26.5°N. *Science* **317**,
979 935–938 (2007).
- 980 **234.** Ferrari, R. & Ferreira, D. What processes drive the ocean heat transport? *Ocean. Model.* **38**, 171 – 186 (2011).

981 **Acknowledgements**

982 L.M. acknowledges funding from the Australian Research Council (grant nos FT180100606 and DP180100048). P.C.T
983 acknowledges funding from the UK Natural Environment Research Council (grant no. NE/R000204/1).

984 **Author contributions**

985 L.M. wrote the manuscript with contributions from L.C.S., L.T. and P.C.T. All authors contributed to the ideas in this paper.

986 **Competing interests**

987 The authors declare no competing interests.

988 **Peer review information**

989 *Nature Reviews Earth & Environment* thanks J. Lynch-Stieglitz, J. Rheinländer, X. Zhang and the other anonymous reviewer(s)
990 for their contribution to the peer review of this work.

991 **Supplementary information**

992 Supplementary information is available for this paper at <https://doi.org/10.1038/s415XX-XXX-XXXX-X>

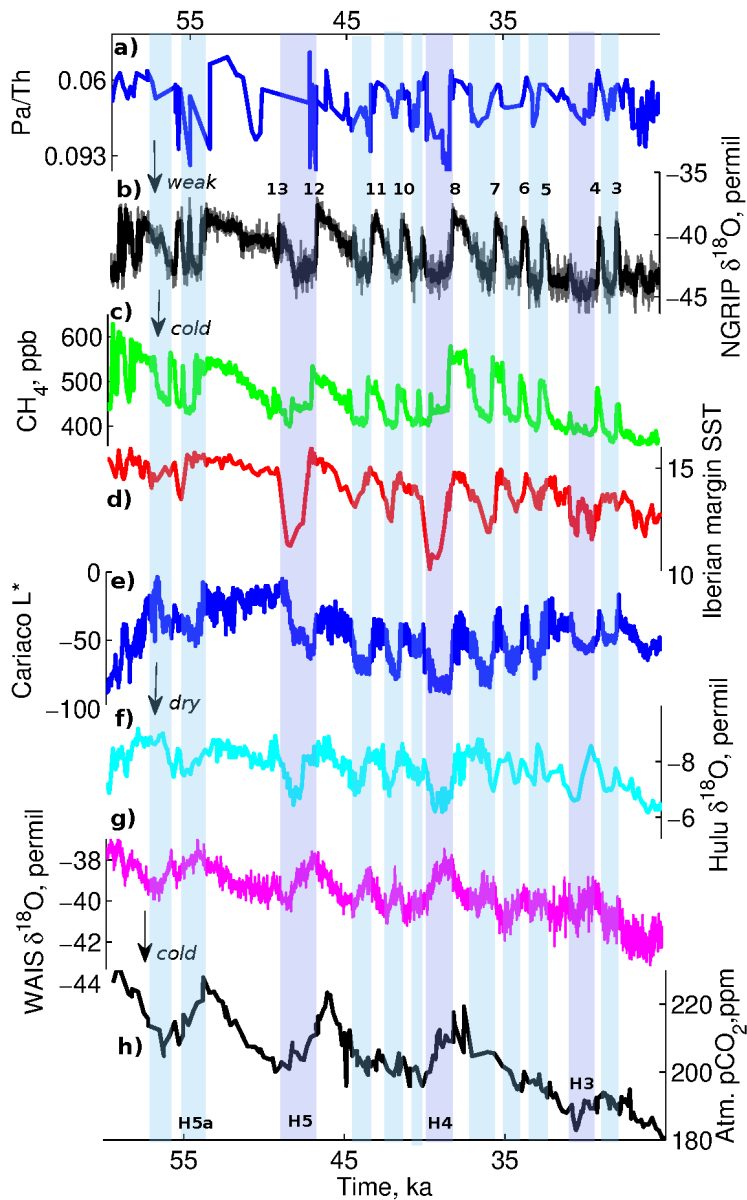


Figure 1. Proxy records showing D–O variability across Marine Isotope Stage 3. **a** | $^{231}\text{Pa}/^{230}\text{Th}$ from the Bermuda rise¹⁰. **b** | North Greenland Ice Core Project (NGRIP) oxygen isotope ratio ($\delta^{18}\text{O}$) on the Greenland ice-core chronology 2005 (GICC05)²²⁹, with the interstadials numbered. **c** | Atmospheric methane (CH_4) concentration from the West Antarctic Ice Sheet (WAIS) Divide ice core¹⁵⁹. **d** | Sea-surface temperature (SST) estimate based on the alkenone unsaturation index (U_{37}^k) from sediment core MD01-2443 retrieved from the Iberian margin²⁶. **e** | Total reflectance (L^*) of sediment from the Cariaco basin⁴⁵. **f** | $\delta^{18}\text{O}$ record from Hulu Cave, China⁴³. **g** | WAIS $\delta^{18}\text{O}$ record⁹⁷. **h** | Atmospheric CO_2 concentration from Siple⁴⁶ and Talos²³⁰ Domes. Blue shading indicates Dansgaard–Oeschger (D–O) stadials, and purple shading indicates Heinrich (H) stadials 5 through to 3. These proxy records show that each stadial is associated with weakening of the Atlantic Meridional Overturning Circulation (AMOC) (panel **a**), cooling over Greenland (panel **b**) and the North Atlantic (panel **d**), low atmospheric CH_4 content (panel **c**), dry conditions in the northern tropics (panel **e**) and a weaker East Asian monsoon (panel **f**), indicating a southward shift of the Intertropical Convergence Zone. D–O stadials are associated with a small $\delta^{18}\text{O}$ increase over Antarctica (panel **g**). Heinrich stadials are associated with an increase in CO_2 (panel **h**) and a more pronounced $\delta^{18}\text{O}$ increase over Antarctica, indicating much warmer conditions. Data for panel **a** from ref.¹⁰. Data for panel **b** from ref.²²⁹. Data for panel **c** from ref.¹⁵⁹. Data for panel **d** from ref.²⁶. Data for panel **e** from ref.⁴⁵. Data for panel **f** from ref.⁴³. Data for panel **g** from ref.⁹⁷. Data for panel **h** from refs.^{46,230}.

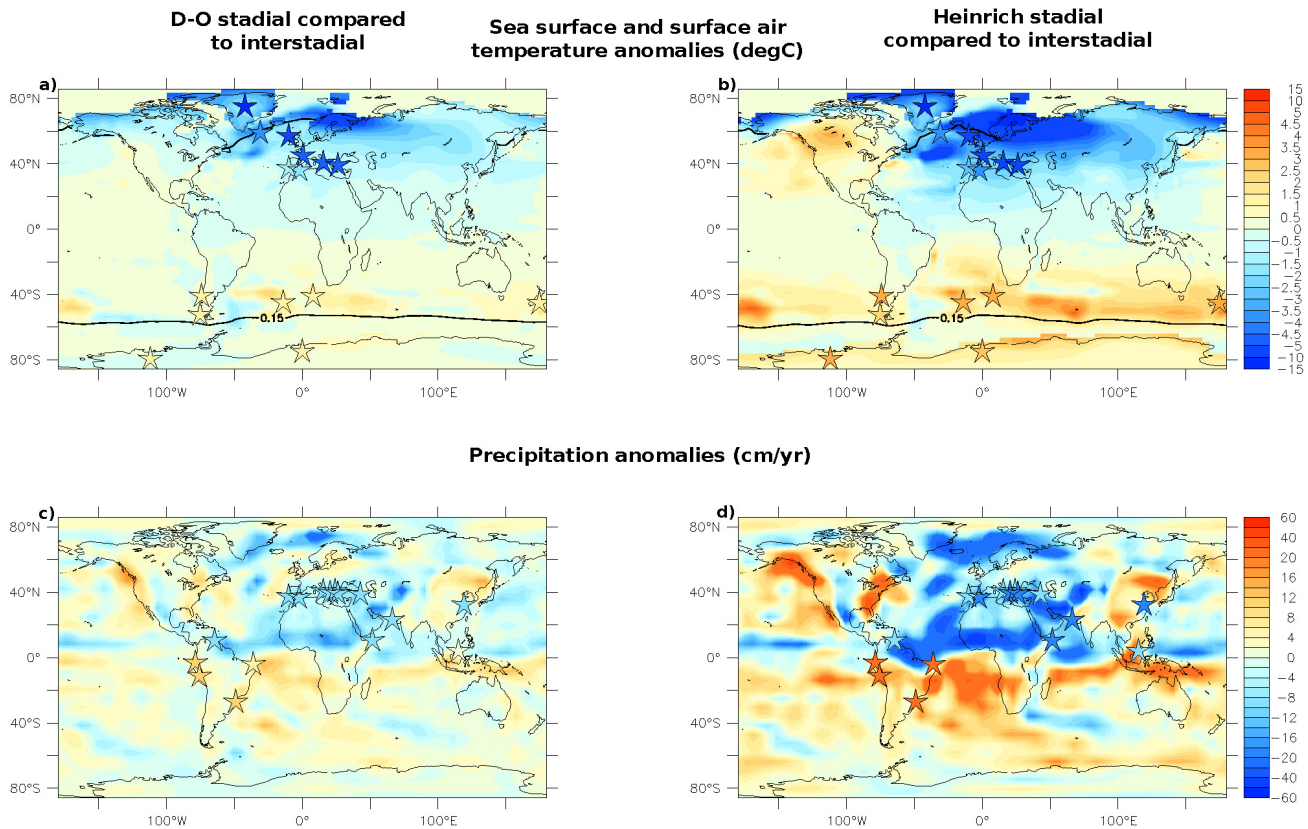


Figure 2. Climatic anomalies associated with D–O and Heinrich stadials compared with an interstadial peak. Stadials are associated with colder and drier conditions in the North Atlantic and Europe, drier conditions in the northern tropics, wetter conditions in the southern tropics and warmer conditions in the South Atlantic. The amplitude of these changes is larger during Heinrich stadials, with notable warming over the Southern Ocean and Antarctica. **a,b** | Annual mean sea-surface temperature (SST) and surface air temperature (SAT) anomalies for a Dansgaard–Oeschger (D–O) stadal (~37.1 ka; panel **a**) and a Heinrich stadal (~39.1 ka; panel **b**) relative to an interstadial peak (~38.1 ka), as simulated in LOVECLIM³⁹. The black line represents the 15% concentration sea-ice contour. **c,d** | Precipitation anomalies for the D–O stadal (panel **c**) and Heinrich stadal (panel **d**) relative to the interstadial peak, as simulated in LOVECLIM³⁹. Stars indicate quantitative (SST) and qualitative (SAT and precipitation) estimates (see Supplementary Tables S1 and S2) of the climatic changes associated with D–O variability of Marine Isotope Stage 3 discussed in the main text.

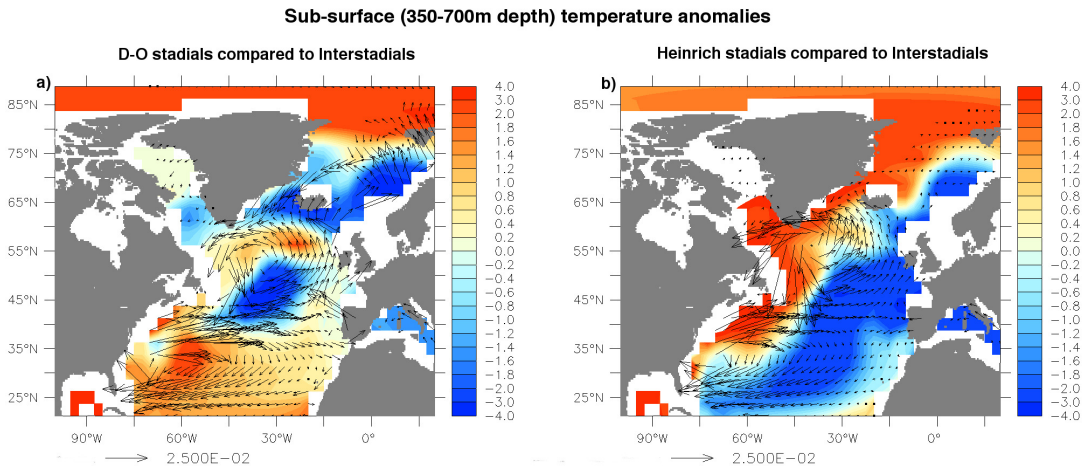


Figure 3. Sub-surface temperature anomalies associated with D–O and Heinrich stadials compared with an interstadial peak. Annual sub-surface (346–694 m depth) temperature anomalies for a Dansgaard–Oeschger (D–O) stadal (~37.1 ka; panel a) and a Heinrich stadal (~39.1 ka; panel b) relative to an interstadial peak (~38.1 ka), as simulated in LOVECLIM³⁹. The sub-surface currents (m s⁻¹), indicated by black arrows, are overlaid.

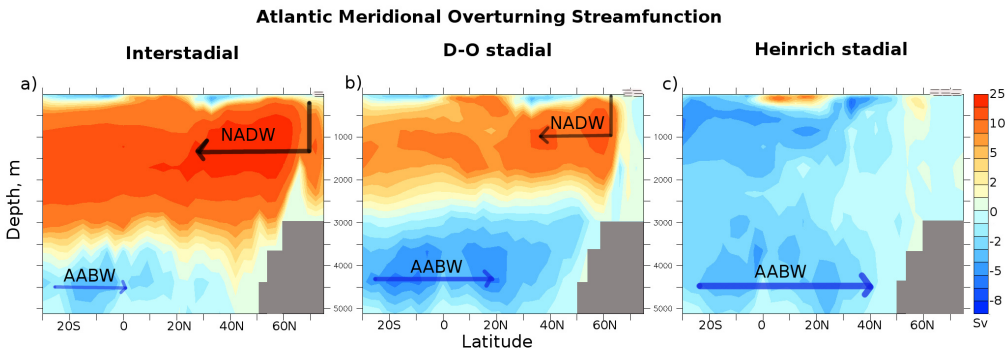


Figure 4. Possible AMOC states for stadials and interstadials. Possible states of the Atlantic Meridional Overturning Current (AMOC) for interstadials (panel a), Dansgaard–Oeschger (D–O) stadials (panel b) and Heinrich stadials (panel c). Positive values indicate a clockwise ocean circulation associated with North Atlantic Deep Water (NADW), whereas negative values indicate an anticlockwise circulation associated with Antarctic Bottom Water (AABW). The grey areas at the surface represent possible winter sea-ice extension in the Nordic Seas.

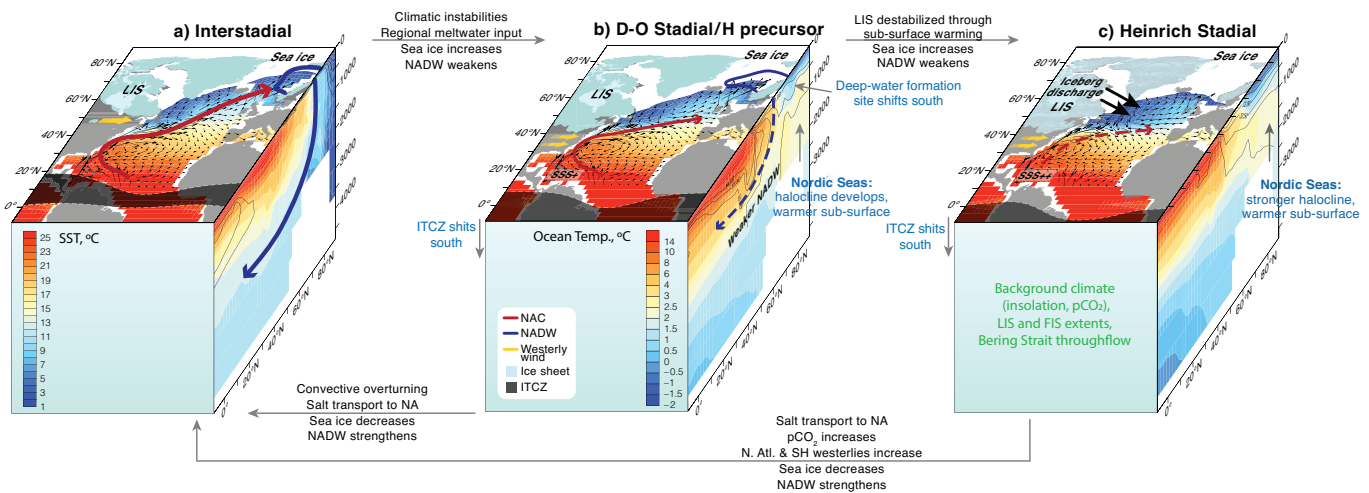


Figure 5. Summary of interactions and feedbacks involved in D–O variability. Schematic of an interstadial peak (panel a), a Dansgaard–Oeschger (D–O) stadial or Heinrich precursor (panel b) and a Heinrich stadial (panel c) showing the possible mechanisms leading to transitions. These schematics qualitatively illustrate the main climatic changes associated with D–O variability, taking into account the large uncertainties associated with quantitative estimates. On going from interstadials to D–O and Heinrich stadials, North Atlantic Deep Water (NADW) formation weakens, deep-water formation sites shift southward, sea-ice extent increases, the annual mean sea-surface temperature (SST) decreases and surface currents (black arrows) are modified, with, in particular, weakening of the North Atlantic Current (NAC). The sub-surface temperature in the northern North Atlantic (NA) increases (the side panel shows the annual mean zonally averaged temperature in the Atlantic with respect to depth and latitude), while a stronger halocline develops (side panel contours). Warmer sub-surface conditions could destabilize the Laurentide ice sheet (LIS) and lead to iceberg discharges in the Hudson Strait, which is characteristic of Heinrich events. As the Atlantic Meridional Overturning Circulation (AMOC) weakens, the Intertropical Convergence Zone (ITCZ) shifts southward, increasing sea-surface salinity in the tropical Atlantic (SSS+). A possible southward extension of the LIS during stadials would intensify North Atlantic westerly winds (yellow arrows). Breakdown of the halocline through convective overturning or increased salt transport to the North Atlantic could lead to a stadial to interstadial transition. Stronger Northern Hemisphere westerlies (arising from LIS changes), Southern Hemisphere (SH) westerlies or increased atmospheric CO₂ concentration during Heinrich stadials could also contribute to AMOC reinvigoration towards an interstadial. Favourable background conditions for D–O variability to occur are indicated in green. FIS, Fennoscandian Ice Sheet.

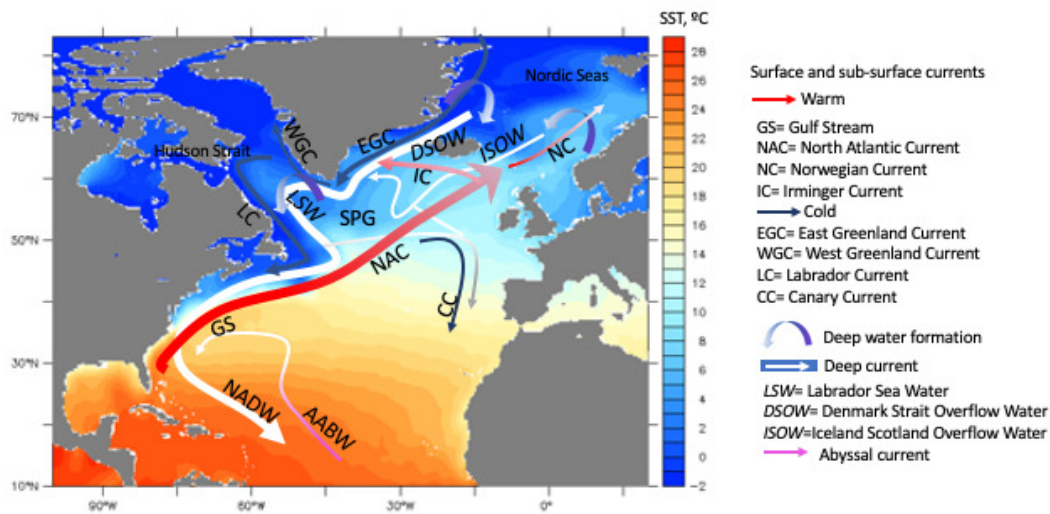


Figure 6. North Atlantic circulation and the AMOC

Box 1 | The AMOC

993 The figure shows the annual mean sea-surface temperature (SST) in the North Atlantic²³¹, as well as the fast-flowing surface
 994 western boundary currents in the Atlantic — the Gulf Stream and its northeast extension, the North Atlantic current — which
 995 bring warm and salty water to the North Atlantic. Subsequent advection of this water to the Nordic Seas, coupled with heat
 996 loss to the atmosphere and sea-ice formation, induces intermediate-depth convection and the formation of North Atlantic
 997 Deep Water (NADW)²³². NADW, one of today’s main deep-water masses, primarily forms in the Nordic Seas with a minor
 998 component in the Labrador Sea¹ and flows southward at a depth of ~1,500–3,500 m in the Atlantic along the deep western
 999 boundary current, below Antarctic Intermediate Waters and above Antarctic Bottom Waters. These water masses, along with
 1000 recirculated deep water from the Indian and Pacific Oceans, mix in the Southern Ocean to form Circumpolar Deep Waters,
 1001 which then flow at depth into the Indian and Pacific Oceans.
 1002

1003 The zonal integral of the surface and deep currents in the Atlantic defines the Atlantic Meridional Overturning Circulation
 1004 (AMOC). Estimating the AMOC transport is a challenge as it requires making measurements across the Atlantic. The RAPID
 1005 Meridional Overturning Circulation and Heatflux Array, established in 2004, has measured an AMOC transport at 26.5°N of
 1006 ~18.7 ± 5.6 Sv (where 1 Sv = 10⁶ m³ s⁻¹), with large seasonal and inter-annual variability²³³. The more recent Overturning in
 1007 the Subpolar North Atlantic Program (OSNAP) observing system, which measures the AMOC over two sections southwest and
 1008 east of Greenland (between 53°N and 59.5°N), reported a mean AMOC transport of 16.8 Sv for the period 2014–2016 (ref.¹).
 1009 The AMOC has a crucial role in heat, freshwater and nutrient transport. The oceanic poleward heat transport at 26.5°N in the
 1010 North Atlantic has been estimated at ~1.3 PW. The AMOC contributes 60–88% of this oceanic heat transport^{78,234}, with the
 1011 remainder being due to the wind-driven gyre circulation. The AMOC strength depends on the density of surface waters in the
 1012 NADW formation region, with the density being a function of salinity and temperature. Dynamical effects, such as the strength
 1013 of the subpolar gyre (SPG), which itself is modulated by North Atlantic wind stress, also affect NADW formation^{216,218}.

1014 **Online summary**

1015 Large changes in Greenland and North Atlantic temperature — termed Dansgaard–Oeschger (D–O) cycles — have been
1016 linked to variations in the strength of the Atlantic Meridional Overturning Circulation. However, the mechanisms are debated.
1017 This Review proposes an oscillatory framework to explain D–O cyclicity, involving atmosphere–ocean–ice interactions.